5-2012

14-3-3 Zeta Overexpression Serves As A Novel Molecular Switch Turning Tgf-Beta From Tumor Suppressor To Tumor Promoter

Jia Xu

14-3-3 ZETA OVEREXPRESSION SERVES AS A NOVEL MOLECULAR SWITCH TURNING TGF-BETA FROM TUMOR SUPPRESSOR TO TUMOR PROMOTER

By
Jia Xu, M.S.

APPROVED:

_____
Dihua Yu M.D., Ph.D.
Supervisory Professor

_____
Varsha Gandhi Ph.D.

_____
Paul Chiao Ph.D.

_____
Peng Huang Ph.D.

_____
Hui-kuan Lin Ph.D.

Approved:

_____
Dean, The University of Texas,
Graduate School of Biomedical Sciences at Houston

14-3-3 ZETA OVEREXPRESSION SERVES AS A NOVEL MOLECULAR SWITCH TURNING TGF-BETA FROM TUMOR SUPPRESSOR TO TUMOR PROMOTER

A
DISSERTATION

Presented to the Faculty of

The University of Texas

Health Science Center at Houston

and

The University of Texas

M. D. Anderson Cancer Center

Graduate School of Biomedical Sciences

in Partial Fulfillment

of the Requirements

for the degree of

DOCTOR OF PHILOSOPHY

By

Jia Xu, M.S.

Houston, Texas

May, 2012

DEDICATION

To my mom:

For her love and support

ACKNOWLEDGEMENTS

First of all, I would like to thank my mentor, Dr. Dihua Yu, for giving me an opportunity to work on such an exciting and important project in her laboratory, and especially for her constant support and guidance during my Ph.D. training. When I first joined her lab, I was still naive in regard to breast cancer biology. After 5 years of training, I have harvested not only my own scientific knowledge but also a sense of what constitutes excellent science. Dr. Yu has constantly challenged me to think logically and hone my presentation skills; both of these lessons have benefited me a great deal. Although I firmly believe that a "running horse needs no spur," I am still grateful for her harshly urging me on my scientific road. Thank you, my "Science Mom." Without you, I would not be here today. I must also thank my former rotation mentors, Dr. Yinhua Yu, Dr. Jean-Pierre Issa, Dr. Shiaw-Yih Lin, who all have given me great scientific guidance during my rotations in their labs. Particularly, I want to thank Dr. Yinhua Yu, who supported me during a successful rotation in my first year in the U.S. with one first author paper and one co-author paper. I could not have imagined that I would have had such a fruitful first-year in the U.S.

I would like to thank Dr. Mien-Chie Hung for scientific inspiration in my academic career. Since joining his Saturday Journal Club, I have been inspired and cheered by every speech he has given, no matter whether it is about scientific thinking and debating, or about how to do science and develop career. Only in such an environment could I have gained such knowledge. Also, at the same time, I learned to be a good presenter and thinker. In addition, he has always supported me to apply for several awards, including my DOD pre-doctoral fellowship, and provided me with a strong recommendation letter.

I would also like to thank my committee members, my Advisory committee: Dr. Wei Zhang, Dr. Angabin Matin, Dr. Menashe Bar-Eli, Dr. Hui-Kuan Lin, as well as my Supervisory committee: Dr. Peng Huang, Dr. Paul Chiao, Dr. Varsha Gandhi, Dr. Hui-Kuan Lin, for their constructive suggestions during each of my committee meetings. I would also like to thank all the staff of GSBS for their excellent work in making GSBS a wonderful training environment.

Special thanks to all the past and present members in Dr. Yu's laboratory, including Chris Danes, Chris Neal, Valerie Hawthorne, Shau-Hsuan Li, Jun Yang, Wen-Chien Huang, Hua Guo, Siyuan Zhang, Jing Lu, Yan Xiong, Yi Xiao, Ozgur Sahin, Patrick Zhang, Frank Lowery, Shanili Jain, Samuel Brady, Sunil Acharya, Sumaiyah Rehman, Brian Pickering, Chia-Chi Tina Chang and Warapen Treekitkarnmongkol, for their friendship and help in the past several years. In addition, I would like to thank Mrs. Ping Li for her tremendous contribution to my paper and extensive technical support, and Dr. Hai Wang for his help analyzing pathology data. I also want to thank Mrs. Irene Shih for her support and help during my Ph.D. I must say I have had a wonderful 6 year Ph.D. journey with these great friends.

Finally, I must thank my parents for their endless love and encouragement. Without their support, it would not have been possible to complete my Ph.D. study. Particularly, I want to thank my dear Mom. She cared for me as best as she could for the 24 years before I came to U.S., She gave me endless support and always believed in me even in the most difficult time of her life. In 2008, the first time she visited the U.S., I suddenly realized she had grown a lot of gray hairs and begun to walk slowly, which I had never noticed previously. From that moment, I felt it was my responsibility to make the rest of her life

honored and joyful. In China, there is an old poem, “谁言寸草心，报得三春晖.” It is my honor to dedicate this Ph.D thesis to my Mom for her 30 years of trust and love to me.

14-3-3 ZETA OVEREXPRESSION SERVES AS A NOVEL MOLECULAR SWITCH TURNING TGF-BETA FROM TUMOR SUPPRESSOR TO TUMOR PROMOTER

Publication No. _____

Jia Xu, M.S.

Supervisory Professor: Dihua Yu, M.D., Ph.D.

TGF-β plays an important role in differentiation and tissue morphogenesis as well as cancer progression. However, the role of TGF-β in cancer is complicate. TGF-β has primarily been recognized as tumor suppressor, because it can directly inhibit cell proliferation of normal and premalignant epithelial cell. However, in the last stage of tumor progression, TGF-β functions as tumor promoter to enhance tumor cells metastatic dissemination and expands metastatic colonies. Currently, the mechanism of how TGF-β switches its role from tumor suppressor to promoter still remains elusive. Here we identify that overexpression of 14-3-3ζ inhibits TGF-β's cell cytostatic program through destabilizing p53 in non-transformed human mammary epithelial cells. Mechanistically, we found that 14-3-3ζ overexpression leads to 14-3-3σ downregulation, thereby activates PI3K/Akt signaling pathway and degrades p53, and further inhibits TGF-β induced p21 expression and cell cytostatic function. In addition, we found that overexpression of 14-3-3ζ promotes TGF-β induced breast cancer cells bone metastatic colonization through stabilizing Gli2, which is an important co-transcriptional factor for p-smad2 to activate PTHrP expression and bone osteolytic effect. Taken together, we reveal a novel mechanism that 14-3-3ζ dictates the tumor suppressor or metastases promoter activities of TGF-β

signaling pathway through switching p-smad2 binding partner from p53 to Gli2. The expected results will not only provide us the better understanding of the important role of 14-3-3ζ in the early stage of breast cancer development, but also deeply impact our knowledge of signaling mechanisms underlying the complex roles of TGF-β in cancer, which will give us a more accurate strategy to determine when and how anti-TGF-β targeted therapy might be effective.

TABLE OF CONTENTS

Approval sheet ..... **i**

Title page ..... **ii**

Dedication ..... **iii**

Acknowledgements ..... **iv**

Abstract ..... **vii**

Table of contents……...**ix**

List of Figures ..... **xii**

Abbreviations ..... **xv**

Chapter 1: Introduction 1

Breast Cancer developmentand progression 1

TGF-β's dual role in cancer development 1

14-3-3 family members in cancer 2

Genetic and epigenetic regulation of 14-3-3σ 3

Chapter 2: Methods and Materials 5

Cell line and cell culture: 5

Antibodies and Reagents: 5

Western blot analysis: 6

Cell proliferation assay, BrdU incorporation assay: 6

Immunoprecipitation: 7

Luciferase reporter assay: 7

mRNA stability assay: 8

Bisulfite genomic sequencing:.....8
5-Aza-2-deoxycytidine treatment:.....10
Protein stability assay:.....10
Generation of knockdown and overexpression cells:.....10
Cytoplasm and nuclear protein fractionation:.....12
Transwell migration assay:.....12
cDNA microarray and analysis:.....13
Wound healing assay:.....13
RNA extraction, RT-PCR (reverse-transcription–polymerase chain reaction) and quantitative real-time RT-PCR:.....13
Osteoblast co-culture assay:.....15
Osteoclast co-culture assay:.....15
Tumor Xenografts and bioluminescence analysis:.....15
X-ray analysis and quantification:.....16
Histomorphometric analysis and immunohistochemical staining:.....16
Statistical analysis:.....17
Chapter 3: Results.....18
14-3-3ζ overexpression inhibits TGF-β cytostatic program in non-transformed human mammary epithelial cells through downregulation of p21.....18
Destabilization of p53 by 14-3-3ζ overexpression suppresses TGF-β induced p21 expression.....27

14-3-3σ downregulation by 14-3-3ζ overexpression contributes to destabilization of p53 in non-transformed HMEC cells. 31

14-3-3ζ overexpression downregulates 14-3-3σ in the early stage of breast cancer development though sequestering YAP1 transcription factor in the cytosol 38

14-3-3ζ overexpression promotes TGF-β induced bone metastatic colonization through activating PTHrP expression 52

Gli2/smad2 complex is required for TGF-β induced PTHrP expression 65

Gli2 stabilization by14-3-3ζ is critical for TGF-β induced PTHrP expression 69

Chapter 4: Discussion 73

TGF-β's function switch. 73

p53's convergence with the TGF-β signaling pathway 75

14-3-3ζ and 14-3-3σ. 77

The complicate role of YAP1 in cancer. 78

Chapter 5: Future studies 80

Bibliography: 83

Vita: 97

LIST OF FIGURES

1: 14-3-3ζ overexpression inhibits TGF-β's cytostatic function in MCF-10A cells. 19

2: 14-3-3ζ overexpression inhibits TGF-β's cytostatic function in MCF-12A cells. 21

3: 14-3-3ζ overexpression switches off TGF-β's cytostatic program through inhibiting p21 expression. 22

4: 14-3-3ζ overexpression switches off TGF-β's cytostatic program, but not through p15 or c-myc 23

5: Knockdown of p21 in MCF-10A cells inhibits TGF-β's cytostatic function. 25

6: p21 is the final executor of TGF-β's cytostatic program in non-transformed human mammary epithelial cells 26

7: Foxo3a does not form a complex with smad4 in response to TGF-β in MCF-10A cells 28

8: p53 forms a complex with smad2 in response to TGF-β in MCF-10A cells 30

9: 14-3-3ζ overexpression leads to downregulation of 14-3-3σ via transcriptional inhibition 32

10: Knockdown of 14-3-3σ inhibits TGF-β's cytostatic function 34

11: 14-3-3σ downregulation contributes to PI3K-Akt activation and p53 destabilization induced by 14-3-3ζ overexpression, thereby contributes to the inhibition of TGF-β's cytostatic program by 14-3-3ζ overexpression 36

12: Rescue of 14-3-3σ in 10A.14-3-3ζ cells recovers the cytostatic function of TGF-β 37

13: 14-3-3σ is upregulated in 14-3-3ζ knockout mice 39

14: 14-3-3ζ and 14-3-3σ are inversely correlated in a panel of

non-transformed HMEC cells and breast cancer cells.....40

15: 14-3-3σ downregulation is independent of p53 regulation in 10A cells 43

16: 14-3-3σ downregulation is not due to promoter methylation.....44

17: 14-3-3σ downregulation is not due to reduced RNA stability

in 10A.14-3-3ζ cells.....46

18: YAP-1 is the transcription factor for 14-3-3σ in 10A cells.....47

19: Knockdown of YAP-1 leads to downregulation of 14-3-3σ in 10A cells 48

20: 14-3-3ζ binds to p-YAP-1 in 10A.14-3-3ζ cells.....50

21: 14-3-3ζ overexpression retains YAP-1 in the cytosol of 10A cells.....51

22: Knockdown of 14-3-3ζ in MDA-MB231 cells.....54

23: Knockdown of 14-3-3ζ in MDA231 cells inhibits cancer cell migration

in response to TGF-β 55

24: Knockdown of 14-3-3ζ in MDA231 cells inhibits cancer cell proliferation in the co-

culture system with MC-3T3 osteoblast cells.....56

25: Knockdown of 14-3-3ζ in MDA231 cells does not change cancer cell proliferation in

response to TGF-β 57

26: Knockdown of 14-3-3ζ in MDA231 cells inhibits osteoclast differentiation in the co-

culture system with Raw264.7 osteoclast cells.....58

27: Knockdown of 14-3-3ζ in MDA231 cells inhibits cancer cell metastatic

colonization in bone microenvironment 60

28: Knockdown of 14-3-3ζ in MDA231 cells inhibits cancer cell metastatic

colonization in the bone microenvironment 61

29: Knockdown of 14-3-3ζ inhibits TGF-β-induced PTHrP gene expression

in MDA231 cells.....63

30: Knockdown of 14-3-3ζ inhibits TGF-β-induced Jagged1 gene expression in MDA231 cells.....64

31: Smad2 binds to Gli2 in MDA231 cells in response to TGF-β treatment 67

32: knockdown of 14-3-3ζ inhibits Smad2 binds to Gli2 in MDA231 cells in response to TGF-β treatment 68

33: Knockdown of 14-3-3ζ dowregulates Gli2 protein level in MDA231 cells in response to TGF-β treatment 70

34: Knockdown of 14-3-3ζ does not change Gli2 mRNA level in MDA231 cells in response to TGF-β treatment 71

35: Schematic diagram depicting 14-3-3ζ-mediated switch of TGF-β function 72

ABBREVIATIONS

ADH	Atypical ductal hyperplasia
DCIS	ductal carcinoma *in situ*
EMT	epithelial mesenchymal transition
GAPDH	glyceraldehyde-3-phosphate dehydrogenase
IP	immunoprecipitation
HCC	non-small cell lung cancer
PI3K	phosphatidylinositol-3 kinase
TGF-β	transformation growth factor-β
TβRI	TGFβ receptor I
TβRII	TGFβ receptor II
PI3K	Phosphatidylinositol 3-Kinase
Akt	Protein kinase B
PTHrP	Parathyroid hormone-related protein
IDC	Invasive ductal carcinoma
HEM	Human epithelial marker
EFP	Estrogen-induced zinc finger protein
IKKα	Inhibitor of nuclear factor kappa-B kinase subunit alpha
Suv39h1	Suppressor of variegation 3-9 homolog family member 1
Dnmt3a	DNA (cytosine-5)-methyltransferase 3A
Gli2	C2H2-type zinc finger protein subclass 2 of the Gli family
YAP1	65 kDa Yes-associated protein 1

TRAP	Tartrate-resistant acid phosphatase
BLI	Bioluminescence imaging

Chapter 1: Introduction

Breast cancer development and progression

The development of breast cancer is a multistep process. Based on epidemiological and histological observations, these steps are defined as a series of morphological and cytological changes from normal epithelium, to ductal hyperplasia, to atypical ductal hyperplasia (ADH), to ductal carcinoma in situ (DCIS), and finally to invasive carcinoma. During this transformation process, there are a multitude of genetic and epigenetic changes accumulated. Currently, the molecular mechanisms underlying this process are still elusive (1, 2). Previously, we discovered that an increase in the expression of 14-3-3ζ begins at ADH, an early stage of breast cancer development, suggesting that 14-3-3ζ overexpression may play an important role in breast cancer initiation (3).

TGF-β's dual role in cancer development

TGF-β plays an important role in differentiation and tissue morphogenesis as well as cancer progression. It has been well characterized that TGF-β binds to its receptor on the cell membrane and induces a signaling cascade by phosphorylating smad2/3. Phosphorylated smad2/3 binds to smad4 and the complex translocates from the cytoplasm to the nucleus to activate the transcription of end effectors, like p15, p21, PTHrP, and others (4, 5). However, the role of TGF-β in cancer is complicated. TGF-β has primarily been recognized as a tumor suppressor because it can directly inhibit cell proliferation or induce apoptosis of normal and premalignant epithelial cells (6). However, in late stage of tumor progression, TGF-β functions as a tumor promoter because it induces an Epithelial-Mesenchymal transition (EMT) increasing the ability of malignant cells to evade immune surveillance and establish metastatic colonies in the second organ sites, (e.g. lung, bone,

liver, and brain) (6). How TGF-β switches its role from a tumor suppressor to promoter remains unsolved in the field. In addition, the importance of TGF-β signaling pathways in cancer has spurred the development of anti-TGFβ compounds that therapeutically target TGF-β and yet fail to show clinical efficacy (7-9). A new paradigm is unraveling in the field of personalized medicine that has shed light on the need to develop biomarkers with which to identify the stage women will most likely show a response to anti-TGFβ compounds, and how to conduct trials using biomarker-guided patient selection and efficacy evaluation.

14-3-3 family members in cancer

The 14-3-3 proteins constitute a family of evolutionarily conserved and ubiquitously expressed proteins in eukaryotic organisms, with seven isoforms in mammals cells denoted as β, γ, ε, η, σ, τ, and ζ (10). These 29-31 kDa acidic proteins bind to specific motifs on target proteins in a phosphorylation-dependent manner (11-14). 14-3-3 proteins function through forming hetero- or homo-dimers to physically interact with specific client proteins and thereby lead to an alteration in these proteins (i.e. sequestration, prevention of degradation, and alteration of enzymatic activity). As a result, 14-3-3 proteins are involved in many cellular processes such as cell-cell adhesion, cell-cycle control, apoptosis, and cell metabolism (11, 13, 15). In fact, the different isoforms have distinct roles in cells. 14-3-3σ is well recognized as a tumor suppressor as a G2/M gatekeeper (16). Conversely, 14-3-3ζ has been identified as an oncogenic isoform and overexpression of 14-3-3ζ is associated with multiple cancer types and regulates various pathways that promote cancer initiation and progression (3). For example, 14-3-3ζ overexpression leads to activation of PI3K-Akt signaling pathway thereby downregulating the tumor suppressor p53 (3, 17). In addition, we have reported that 14-3-3ζ is overexpressed in >40% of advanced stage breast cancers and

has a strong correlation with disease recurrence and poor survival in breast cancer patients (18). In addition, we have found that 14-3-3ζ overexpression can promote breast cancer progression from early stage (DCIS) to late stage (IDC) via Epithelial-Mesenchymal Transition (EMT) through binding and stabilizing TGFβR1 and activating TGF-β pathway (19). These lines of evidence strongly suggest that deregulation of 14-3-3 proteins may play an important role in cancer initiation and progression and may be a potential target for developing anticancer therapeutics.

Genetic and epigenetic regulation of 14-3-3 σ

Among the 14-3-3 family, 14-3-3 σ, also known as human epithelial marker (HEM) or stratifin, is well recognized as a tumor suppressor gene, and is lost in multiple types of cancer. The expression of 14-3-3σ can be regulated by different mechanisms. 14-3-3σ is regulated by another tumor suppressor gene, p53, which is strongly induced by ionizing radiation and DNA damage. p53 is dephosphorylated and activated following cellular DNA damage, and it then binds to the promoter region of 14-3-3σ, and leads to increased transcription of 14-3-3σ and G2/M arrest (16, 20). 14-3-3σ expression in basal/progenitor cell may be repressed by ΔNp63, a dominant negative isoform which can suppress both p53 and TAp63 transactivation (21-23). Moreover, 14-3-3σ can be regulated by estrogen-induced zinc finger protein (EFP). In breast epithelial cells, EFP acts as an E3 ligase to ubiquitinate 14-3-3σ that is then quickly degraded (24).

Gene silencing of 14-3-3σ, mainly modulated by CpG methylation in the promoter region, occurs in several types of solid tumor, including prostate, lung, breast, skin cancer, and also in hematologic malignancies (25-31). Epigenetic inactivation of 14-3-3σ is a very early event in carcinogensis and the extent of 14-3-3σ promoter hypermethylation gradually

increases from the early stage to late stage during the breast cancer progression, (i.e. atypical hyperplasia (38%), ductal carcinoma in situ (83%), and invasive ductal carcinoma (96%)) (28). Although p53 and ΔNp63 have been reported to be the major regulator of 14-3-3σ expression in cell lines, no association between 14-3-3σ expression and p53 mutations or increased level of ΔNp63 was seen in human tissue, suggesting that the constitutive expression of 14-3-3σ may be dependent on factors other than p53 (32, 33). Recently, IKKα was found to be an important transcription factor of 14-3-3σ, as it can directly prevent Histone H3-K9 trimethylase Suv39h1 and Dnmt3a access to 14-3-3σ promoter, thereby preventing hypermethylation of 14-3-3σ (34).

Chapter 2: Methods and Materials

Cell line and cell culture:

MCF-10A cell line was a kind gift from Dr. Robert Pauley (Karmonos Cancer Institute, Detroit, MI), and was cultured in MCF-10A medium : Dulbecco's Modified Eagle's Medium (DMEM, Caisson Labs) supplemented with 5% Horse Serum (Invitrogen, CA), 20ng/ml epidermal growth factor (EGF), 10 μg/ml insulin, 0.5 μg/ml hydrocortisone (Sigma-Aldrich, MO), 100 ng/ml cholera toxin (Calbiochem, Darmstadt, Germany). MCF-12A, MDA-MB-231 cell lines were obtained from American Type Culture Collection (ATCC). MCF-10A and MCF-12A cell lines and their genetically modified variants were maintained in MCF-10A medium. MDA-MB-231 cell line and its genetically modified variants was maintained in DMEM with 10% FBS and antibiotics. The murine osteoblast cell line MC3T3 was a kind gift from Dr. Sue-Hwa Lin (Department of Molecular Pathology, M.D. Anderson Cancer Center), and was maintained in growth medium αMEM supplemented with 10% FBS and antibiotics. The murine pre-osteoclast cell line RAW 264.7 was a kind gift from Dr. Bharat B. Aggarwal (Department of Experimental Therapeutics, M.D. Anderson Cancer Center), and was maintained in DMEM with 10% FBS and antibiotics for regular culture and supplemented with 30ng/ml RANKL for osteoclastogenesis assays.

Antibodies and Reagents:

Antibodies for 14-3-3ζ (sc-1019), p53 (sc-126) , smad4 (sc-7966), Lamin B (sc-6217) were purchased from Santa Cruz Biotech; 14-3-3σ (ab14123), Gli2 (ab7195) antibodies were purchased from Abcam; Foxo3a (07-102) antibody was purchased from Millipore; p21 (610234) antibody was purchased from BD Transduction Laboratories; β-actin (A2172) and

tubulin (T6199) antibodies were purchased from Sigma-Aldrich; p-Akt (4058), T-Akt (9272), T-smad2/3(3102), p-YAP1 (4911), T-YAP1 (4912), smad2 (3122), smad3 (9513), p-smad2 (3101) and p-smad3 (9520) antibodies were purchased from Cell Signaling Technology; antibody for p53(OP03, Calbiochem) and smad2 were used for immunoprecipitation assay as previously described(35). Recombinant Human TGFβ1(4342-5) was purchased from BioVison, and diluted in 1xPBS at 5ng/ml concentration; TGF-β Receptor 1 kinase inhibitor (LY2109761, Eli Lily) was kindly provided by Eli Lily through collaboration.

Western blot analysis:

Total cell lysates were collected with immunoprecipitation (IP) lysis Buffer (20 mM Tris [pH 7.5], 150 mM NaCl, 1 mM EDTA, 1 mM EGTA, 1% Triton X-100, 2.5 mM sodium pyrophosphate, 1 mM beta-glycerolphosphate, 1 mM sodium orthovanadate,1 mM PMSF and protease inhibitor cocktail). Whole cell lysates were obtained by sonication followed by centrifugation. Protein concentration was measured by BCA protein assay kit (Pierce). Equal amounts of cell lysates were subjected to electrophoresis using SDS-PAGE and transferred to Polyvinyldifluoride membrane (Bio-Rad). Membranes were blocked with 5% milk (in PBS-T) for 30 min, followed by primary antibody incubation overnight at $4^{o}C$, and after three washes with PBST (5 min each), incubated with secondary antibody (5%milk in PBS-T) for 60 min, and signal was detected by ECL (Amersham) following the manufacturer's instructions.

Cell proliferation assay, BrdU incorporation assay:

Cells were plated at 1 x 104 cells/plate in triplicate in 10 cm cell culture plates for both control and TGF-β treatment (5ng/ml). At each time point (24, 48 and 72 hrs), cells were

trypsinized and live cells were counted using hemocytometer. BrdU incorporation assay was performed following instruction of BrdU Cell Proliferation Kit (Millipore) after treatment with TGF-β (5ng/ml) or vehicle. The percentage of cell proliferation was calculated after 72 hours treatment and normalized to the group without treatment.

Immunoprecipitation:

Cell lysates were prepared as previously described. Cell lysates (1000μg) were diluted with IP buffer, and then pre-cleared by incubation with 2μg of isotype matched IgG and 35 μl protein G-linked agarose beads (Roche Diagnostic) for 2 hour at 4^{o}C. After pre-clearing lysates were incubated with 1 μg specific antibody overnight at 4^{o}C, followed by incubation with 50μl protein-G linked agarose beads for 1 hour. The beads were then pelleted at 1000 rpm and washed with cold IP buffer for three X 10 min. The washed immunoprecipitated complex was mixed with 2X loading buffer (100 mM Tris-HCL [pH 6.8], 200 mM DTT, 4% SDS, 0.2% Bromophenol blue, 20% glycerol) at a 1:1 ratio and denatured by boiling for 5 min, followed by western blot analysis with specific antibodies as described previously.

Luciferase reporter assay:

Genomic DNA was extracted from MCF-10A parental cells (Purelink Genomic DNA mini kit, invitrogen) and used as template to clone the 14-3-3σ promoter fragment with the following primers: 741 forward 5'-GGCCTGGAGGATGGAACC-3'; 922 forward 5'-CAACTTGAAAGGGAAATTGTGTAG-3'; 1221 forward 5'-CATCACGTAGCTGGAATTGCTG-3'; shared reverse 5'-TCTCCTCCGAGCCCTCCT-3' as indicated in Figure 16. The PCR product was then cloned into pGL3 luciferase vector to generate sequential deletion mutations of pGL3.14-3-3σ luciferase reporter. For specific transcription factor binding site mutations in 181 bp promoter region, the following primers

for M1: F1: 5'-AAGGGAAAATTGTGTAGTAAAAAAAATGTG-3', R1: 5'-GGTTTGTTGGACACATTTTTTTTTACTACAC-3'; M2: F2: 5'-CCAACAAACCTACTGGGTAAAAAAAAAAAAAGGCTGG-3', R2: 5'-GCTCCAGCCCAGCCTTTTTTTTTTTTTACCCAGTA-3'; M3: F3: 5'-GCACTCTGAAAGCTGCCAAAAAAACATTCTGG-3', R3: 5'-CCCTCTGAGCTCCCAGAATGTTTTTTTGGCAGC-3'; M4: F4: 5'-GCTCAGAGGGGACCCTGAAAAAAAATGAGG-3', R4: 5'-CCATCCTCCAGGCCTCATTTTTTTTCAGGGTCCC-3'; M5: F5: 5'-GCGCATTCTGGGAGCTCAAAAAAAACCCTGAG-3', R5: 5'-CCTCATTCCCCCTCAGGGTTTTTTTTGAGCTCC-3'; were used to generate the mutated clones. Luciferase reporter plasmids were co-transfected into target cells with Renilla-Tk luciferase vectors (Promega) as transfection efficiency control by Amaxa Nucleofector transfection with program T-24. After 48 hours, the reporter luciferase activity was measured and normalized to control Renilla luciferase activity by Dual-Luciferase Reporter Assay system from Promega following the manufacturer's instructions.

mRNA stability assay:

Equal numbers of cells were plated in 10-cm plates and incubated at 37°C until they reached 70% confluence. Cells were treated with 5 μg/ml antinomycin D for 0, 1, 2, or 4 hours. Total RNA was extracted with TRIzol reagent (Invitrogen, San Diego, CA), and qRT-PCR analysis was performed to determine the relative mRNA level of 14-3-3σ.

Bisulfite genomic sequencing:

Dilute 1-2 μg genomic DNA extracted from MCF-10A.vec or MCF-10A.14-3-3ζ cells into 50μl distilled H2O. Add 5.5μl of 2M NaOH and incubate at 37°C for 10 minutes to

create single stranded DNA. At the same time, freshly prepare 10mM hydroquinone (sigma) buffer (55 mg hydrochinone in 50 ml of water) and add 30µl into DNA. Add 520µl freshly prepared 3M sodium bisulfite(sigma s-8890) solutions: mix 1.88g of sodium bisulfite with 5 ml of water and adjusting pH to 5.0 with NaOH. Incubate DNA mixture at 50°C for 16 hours. Use DNA wizard cleanup kit (Promega A7280) to recover DNA, and Resuspend in 50µl TE buffer, and mix well. Desulfonate the DNA by adding 5.5µl of 3M NaOH and incubating at room temperature for 5 mins. Precipitate DNA by adding 1µl glycogen (Boehringer) as carrier, 33µl of 10M NH4Ac, and 3 volumes of ethanol. Incubate overnight at -20°C, then mix and centrifuge DNA for 30 mins at 4°C. Wash pellet in 70% ethanol and then air dry (as described above) and resuspend in 50µl TE buffer. At this stage the sample can be kept in the refrigerator over night.

Methylation status was analyzed by bisulfite genomic sequencing of both strands of the corresponding CpG islands. Ten independent clones for each sample were analyzed. The bisulfite-modified DNA was then amplified by methylation-specific PCR using primer pairs that specifically amplify two regions of 14-3-3σ promoter. A 580bp sequence containing 7 CpG dinucleotides (Figure 1A) was amplified using Sigma-MR1 (5'-AACAACACCCTCCAAACAACC-3') and Sigma-MF1(5'-GGAAGGGTATTGTGAAAGTGGA-3'); A 770bp sequence containing 20 CpG dinucleotides was amplified using Sigma-MR2 (5'-AAAACCTCCCACCCCATACT-3') and Sigma-MF2 (5'-TGAGGATATGGTAGTTTTTATGAAAGG-3'). Cycling conditions were: 95°C/5 min × 1 cycle; 95°C/45 sec, 59°C/30 sec, 72°C/30 sec × 31 cycles; 72°C/5 min × 1 cycle. Gel extracted PCR products were subcloned into pCR2.1-Topo vector (Topo TA cloning kit, Invitrogen, Carlsbad, CA) and transformed into competent DH5α *Escherichia*

coli cells (Invitrogen). Plasmid DNA was purified with Qiagen Maxi or Midi kits (Qiagen, Valencia, CA) and sequenced using universal T3 and/or T7 primers. Sequencing was performed by the MDACC core facility.

5-Aza-2′-deoxycytidine treatment:

MCF-10A sublines were treated with 0, 2.5, or 5 μM of the hypomethylating reagent 5-aza-2-deoxycytidine (DAC; Sigma, St. Louis, MO) respectively. Fresh DAC was added daily for 5 days, after which cell lysates were collected for western blot analysis.

Protein stability assay:

MG-132 (10 μM; Calbiochem) was given to the target cells to inhibit proteasome-mediated protein degradation as previously described (3). Cell lysates are collected at the time points of 4, 8, or 16 hours and western blot analysis of p53, p21, 14-3-3σ and 14-3-3ζ protein level. β-actin was used as a loading control.

Generation of knockdown and overexpression cells:

Stable shRNA-mediated knockdown was achieved with the pLKO.1-puro system (MISSION RNAi, Sigma-Aldrich) targeting two coding sequence: shRNA535 (CCGGGACAGATTTCTACCACTCCAACTCGAGTTGGAGTGGTAGAAATCTGTCTT TTTG); and shRNA233 (CCGGGAGCGATGGAACTTCGACTTTCTCGAGAAAGTCGAAGTTCCATCGCTCTT TTTG) for p21. shRNA lentiviral vectors were transfected into the packaging cell line 293T together with two other plasmids: packaging DNA (psPAX2) and envelope DNA (pMD2G) through Lipofectamine transfection. After 48 hours viruses were collected, filtered and used to infect target cells in the presence of 8-10μg/ml polybrene for 24 hours. The infected MCF-10A cells were selected with 2μg/ml puromycin. To stably knockdown 14-3-3σ, two

14-3-3σ shRNA lentiviral plasmids (RefSeq NM_006142, Sigma-Aldrich) targeting 14-3-3σ 3'-UTR and coding sequence were used in the experiments: shRNA128 (CCGGCTGCCTCTGATCGTAGGAATTCTCGAGAATTCCTACGATCAGAGGCAGTTTTTG); and shRNA130 (CCGGGACGACAAGAAGCGCATCATTCTCGAGAATGATGCGCTTCTTGTCGTCTTTTTG). For stable knockdown of 14-3-3ζ in the MDA231 breast cancer cell line, three shRNA clone (RefSeq NM_003406) were purchased from Sigma-Aldrich targeting the coding sequence: shRNA4 (CCGGGCAGAGAGCAAAGTCTTCTATCTCGAGATAGAAGACTTTGCTCTCTGCTTTTT); shRNA5 (CCGGGCAATTACTGAGAGACAACTTCTCGAGAAGTTGTCTCTCAGTAATTGCTTTTT); and shRNA8 (CCGGCTCTGTGTTCTATTATGAGATCTCGAGATCTCATAATAGAACACAGAGTTTTT). Viruses were generated and used to infect target cells as above and then subsequently selected with 3μg/ml puromycin in MDA231 cells. Control cell lines were derived from parental vector alone.

For stable knockdown of YAP1, three Lentiviral shRNAs targeting the YAP-1 coding sequence were purchased from Open Biosystems: shRNA2 (TGCTGTTGACAGTGAGCGCTAGCTCAGATCCTTTCCTTAATAGTGAAGCCACAGATGTATTAAGGAAAGGATCTGAGCTATTGCCTACTGCCTCGGA); shRNA3 (TGCTGTTGACAGTGAGCGCCCATTGCTGCTGTTAATGTATTAGTGAAGCCACAGATGTAATACATTAACAGCAGCAATGGATGCCTACTGCCTCGGA); and shRNA4 (TGCTGTTGACAGTGAGCGCGCAATCACTGTGTTGTATATATAGTGAAGCCACAG

ATGTATATATACAACACAGTGATTGCATGCCTACTGCCTCGGA). For stable overexpression of 14-3-3σ in the MCF-10A.14-3-3ζ and MCF-10A.14-3-3ζ.ErbB2 cells, the coding sequence was subcloned from pCMV-SPORT6-14-3-3σ (Openbiosystems) into the lentiviral expression vector pENTR3C-GFP vector (Invitrogen) to allow for Kanamycin antibiotic selection. Finally, it was subcloned into lentiviral vector pLove-14-3-3σ-GFP for lentiviral infection. Stable overexpression cell lines were generated as above.

Cytoplasm and nuclear protein fractionation:

Cells were trypsinized, centrifuged at 1000 rpm, and then washed with PBS. The cell pellet was resuspended with hypotonic buffer (10 mM HEPES [pH 8.0], 1.5 mM MgCl2, 10 mM KCl, 1 mM PMSF and protease inhibitor cocktail) and incubation on ice for 15 min. Centrifuge at 10,000rpm at 4^{o}C for 5 min to pellet cells. The pellet was then resuspended with buffer containing 10 mM HEPES [pH 8.0], 1.5mM $MgCl_2$, 10 mM KCl and 0.05% NP-40, and incubated on ice for 30 min. Cytoplasmic fractions were separated by 50 strokes of a dounce homogenizer (type B pestal). Extracts were centrifuged at 13,000 rpm at 4^{o}C for 10 min and the supernatant was retained as cytoplasmic fraction. The nuclear pellet was washed twice with hypotonic buffer and then pelleted, resuspended with nuclear extract buffer (10 mM HEPES [pH 8.0], 1.5 mM MgCl2, 400 mM NaCl, 0.1 mM EDTA, and 20% Glycerol), followed by incubation on ice for 30 min. A 30-guage syringe was used to break up the pellet and release nuclear protein. Extracts were centrifuged at 13,000 rpm at 4^{o}C for 15 min, and the supernatant was retained as the nuclear fraction.

Transwell migration assay:

231.Vec, 231.σ and 231.ζ cells (1×10^5 cells/chamber) were resuspended in DMEM and added to the top chambers of 24-well transwell plate (Costar, 8-μM pore size). The bottom

chamber was filled with 10% FBS containing DMEM (with or without TGF-β) as an attractant. After 12 hours of incubation, non-migrated cells on the top side of membrane were removed by swiping with Q-tips. The migrated cells on the bottom side of the membrane were fixed with 20% methanol and stained with crystal violet for visualization. The number of migrating cells in three fields from each well was counted under 20X magnifications.

cDNA Microarray and analysis:

Two unbiased platforms were applied to gene profiling of MCF-10A.14-3-3ζ cells compared to MCF-10A.Vec and parental cells: one is Human Genome U133 Plus 2.0 Array (Affymetrix), which offers comprehensive analysis of genome-wide expression on a single array; another one is Whole genome 44K long oligo array (Agilent) in collaboration with the cDNA microarray core facility at UT-MDACC. Microarray data were analyzed by using Gene Ontology software online (http://bioinfo.vanderbilt.edu/gotm/), and hierarchical cluster analysis algorithms and graphical representation of the data were performed by aligning our microarray data with the other cDNA microarray data from 19 normal breast tissue samples and 43 breast cancer patient samples online using Cluster and Treeview software.

Wound healing assay:

Cells were grown to confluence in a 6-well plate, and then scratched using a 200 μL sterile pipette tip. Images of wounded monolayers were photographed under an inverted microscope at the time of wounding (0 h) and 6 h later.

RNA extraction, RT-PCR (reverse-transcription–polymerase chain reaction) and quantitative real-time RT-PCR:

Total RNA from cells was isolated using Trizol reagent (Invitrogen) and protocol was followed as per the manufacturer's instructions. 1 µg of total RNA was reverse transcribed to cDNA using iScript™ cDNA synthesis kit (Biorad) following the manufacturer's instructions. Then, an equivalent volume (1 µl) of cDNA was used as template for quantitative real-time PCR with iQ™ SYBR Green Supermix (Biorad) and the StepOnePlus™ (Applied Biosystems) instrument according to the manufacturer's instruction. The name of the gene quantified and the sequence of the primers are given in the following table. The threshold cycles for specific targets were then normalized to the threshold cycles of GAPDH to calculate the relative fold change difference.

Primers:

gene	Primers
P21	F: 5'-GTCACTGTCTTGTACCCTTGTG-3' R: 5'-CGGCGTTTGGAGTGGTAGAAA-3'
P15	F: 5'-CGTGCTGACATCTATGCAAT-3' R: 5'-AGCTGCTCCATTGGCATAC-3'
c-myc	F: 5'-CCTGGTCAAGAAGCATTTCAA-3' R: 5'-GCCCCAAAGATGAGGAGTATC-3'
14-3-3σ	F: 5'-TTCTTCTGCGCTACTGCTGCG-3' R: 5'-GGGCAGGTATGGAGAGGAAGA-3'
Gli2	F: 5'-AGTTTGTTCTCGGGTGCTCTG-3' R: 5'-ACATCTGTCATCTGAAGCGGC-3'
GAPDH	F: 5'-TGGTATCGTGGAAGGACTCATGAC-3' R: 5'-ATGCCAGTGAGCTTCCCGTTCAGC-3'
Jagged1	F: 5'- GAGCTATTTGCCGACAAGGC-3' R: 5'- GGAGTTTGCAAGACCCATGC-3'

IL-11	F: 5'-CTCGAGTTTCCCCAGACC-3' R: 5'-GTCAGCTGGGAATTTGTCC-3'
PTHrP	F: 5'-TTTACGGCGACGATTCTTCC-3' R: 5'-TTCTTCCCAGGTGTCTTGAG-3'

Osteoblast co-culture assay:

MC3T3 cells (3×10^4 cells/well) were seeded in 6-well plates. After confluence was achieved, Luciferase/GFP-labeled (GFP^+) 231.scramble, 231.ζKD4, 231.ζKD5, 231.Vec, 231.σ or 231.ζ cells (1×10^4 cells/well) were added on top of MC3T3 cell layer in triplicate and treated with or without 5ng/ml TGF-β. The co-culture assays were performed in α-MEM medium supplemented with 10% FBS and changed every two days. After 6 days the co-culture was subjected to a luciferase assay to quantify the relative number of tumor cells. These values were normalized against luciferase quantification of 6-well plates seeded with tumor cells alone.

Osteoclast co-culture assay:

231.scramble, 231.ζKD4, 231.ζKD5, 231.Vec, 231.σ or 231.ζ cells (1×10^4 cells/well) were mixed with murine pre-osteoclast RAW 264.7 cells (3×10^4 cells/well) in medium containing 30 ng/ml RANKL, and seeded into 6-well plates together. The co-cultures were performed in DMEM medium supplemented with 10% FBS and changed every two days. TRAP staining was performed on day six using a leukocyte acid phosphatase kit (Sigma). TRAP+-multinucleated cells were scored as mature osteoclasts. The number of nuclei per osteoclast was quantified using TRAP-stained images.

Tumor Xenografts and Bioluminescence Analysis

All procedures involving mice and experimental protocols were approved by the Institutional Animal Care and Use Committee (IACUC) of University of Texas M.D. Anderson Cancer Center. For bone metastasis studies, $2X10^5$ tumor cells were injected into the bone of anesthetized female athymic Ncr-nu/nu mice. Development of bone metastases was monitored by bioluminescence imaging (BLI). Anesthetized mice were retro-orbitally injected with 75mg/kg D-Luciferin. Bioluminescence images were acquired with a Xenogen IVIS 200 imaging system. Analysis was performed with live imaging software by measuring photon flux in the hindlimbs of mice. Data were normalized to the signal on day 21. Bone metastasis-free survival curves represent the time point at which each mouse developed bone metastasis by threshold BLI signals in the hindlimbs.

X-ray analysis and quantification:

Osteolysis was assessed by X-ray radiography. Anesthetized mice were exposed to X-ray radiography at 40 mm for 1 min and directly imaged by Carestream Molecular Imaging software using Kodak In-Vivo Multispectral Imaging system. Osteolytic lesions were identified on radiographs as demarcated radiolucent lesions in the bone and quantified using ImageJ software (National Institutes of Health).

Histomorphometric analysis and immunohistochemical staining

Hindlimb bones were excised from mice at the end point of each experiment, and fixed in 10% neutral-buffered formalin, decalcified in 10% EDTA for 2 weeks, and embedded in paraffin for hematoxylin and eosin (H&E), tartrate-resistant acid phosphatase (TRAP) (Kos et al., 2003), or immunohistochemical staining. Histomorphometric analysis was performed on H&E stained bone metastasis samples using the Zeiss Axiovert 200 microscope and AxioVision software version 4.6.3 SP1. Immunohistochemical analysis was performed with

heat-induced antigen retrieval. Primary antibodies used were anti-14-3-3ζ (Santa Cruz, sc-1019) and anti-14-3-3σ (abcam, ab14123). Biotinylated secondary antibody was used with Vectastain ABC Kit (Vector Laboratories) and DAB detection kit (Zymed) to reveal the positively stained cells with nuclei counterstained with hematoxylin.

Statistical analysis:

Statistics were performed using log rank test, chi-square test, or student t-test. $p<0.05$ was considered significant.

Chapter 3: Results

14-3-3ζ overexpression inhibits TGF-β cytostatic program in non-transformed human mammary epithelial cells through downregulation of p21

TGF-β controls a large number of genes through immediate effects on transcriptional activation and repression (5, 6, 36). These effects are primarily mediated by the smad2/3 complex which are directly activated by TGF-β and translocate from the cytoplasm to the nucleus (36). In normal epithelial cells, TGF-β induces a cytostatic program involving two classes of immediate gene responses (5). One class includes genes encoding the cyclin-dependent kinase (cdk) inhibitors p15(37) and p21 (38) (39, 40) which inhibit cell cycle progression. The other class includes genes that promote cell growth, like c-myc(41) (42, 43), and Id1/2/3(44) . The two different readouts could be due to the smad2/3 complex binding together with different transcriptional partners to either repress (E2F4/5 and p107 or ATF3) or activate (p53 or FOXO3a) gene expression. However, in the late phase of tumor progression, the major function of TGF-β is to induce EMT through transcriptional upregulation of numerous factors, including SNAIL1(45), HMGA2 (46), ZEB1 (47) and ZEB2 (SIP1)(48). These factors are crucial for repressing E-cadherin and other tight junction molecules. TGF-β and 14-3-3ζ are known to corporately affecting cell proliferation and tumorigenesis. However, the critical regulatory mechanism linking 14-3-3ζ to the TGF-β signaling pathway in breast cancer initiation and progression remains unclear. To address this question, we have stably introduced 14-3-3ζ into the non-transformed MCF10A Human Mammary Epithelial cells (HMEC) and established the 14-3-3ζ overexpressing stable line MCF-10A.14-3-3ζ (Fig.1c).

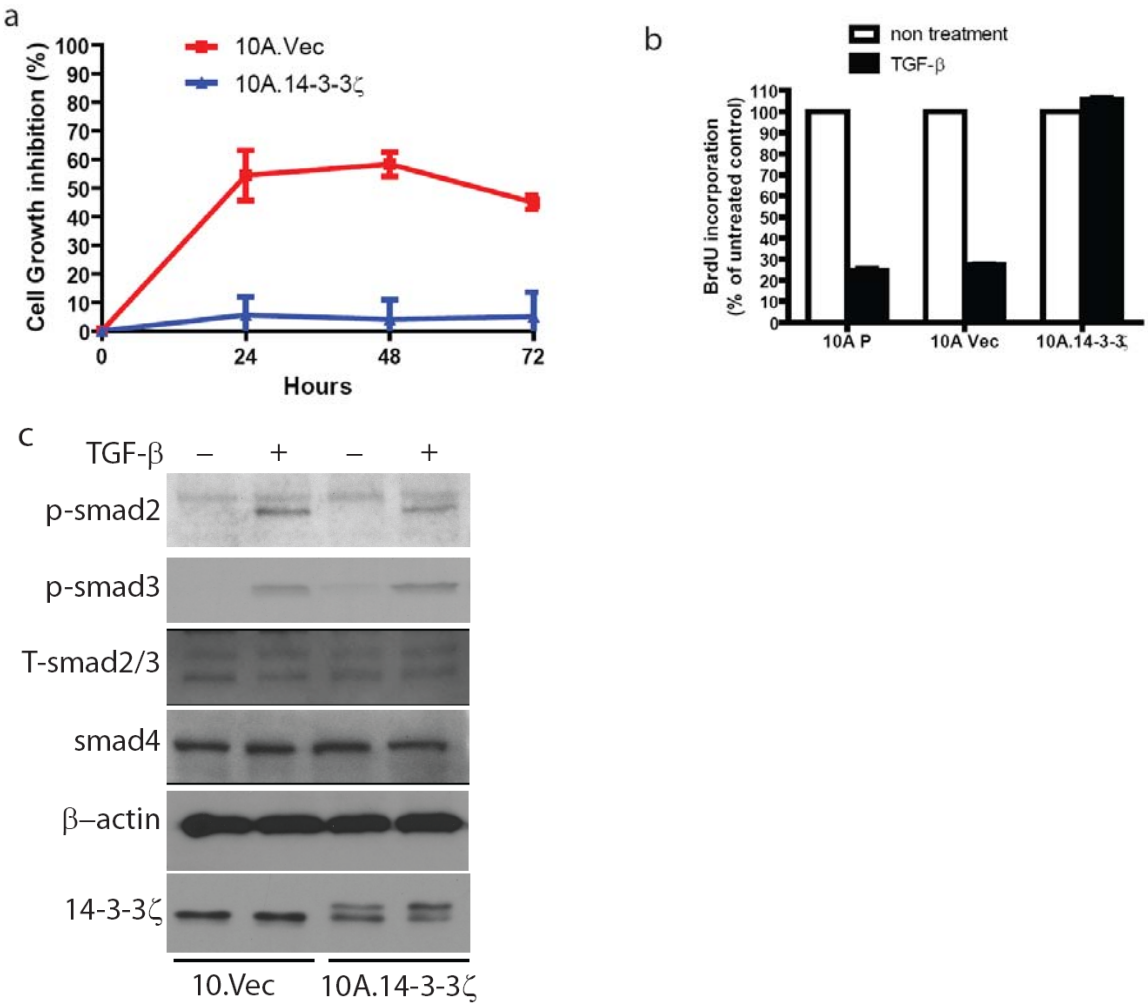

Figure 1. 14-3-3ζ overexpression inhibits TGF-β's cytostatic function in MCF-10A cells. a) MCF-10A.Vec or MCF-10A.14-3-3ζ cells were treated with TGF-β (5ng/ml) or vehicle. Cells were counted every 24 hours and plotted as percent inhibition relative to vehicle control. b) BrdU incorporation assay in MCF-10A parental cell, MCF-10A.Vec and MCF-10A.14-3-3ζ cells treated with TGF-β (5ng/ml) or vehicle. The percentage of cell proliferation was calculated after 72 hours treatment and normalized to the group without treatment. c) Western blot analysis of TGF-β signaling pathway in MCF-10A.Vec and MCF-10A.14-3-3ζ with or without TGF-β treatment for 2 hours.

Our lab has previously published that 14-3-3ζ stabilizes TGFβRI and promotes the TGF-β induced EMT program in MCF-10A.14-3-3ζ cells through SIP1/ZEB2, a repressor of E-cadherin (19). Interestingly, I found that 14-3-3ζ in MCF-10A cells not only promotes EMT, but also simultaneously blocks the cytostatic program induced by TGF-β making 10A.14-3-3ζ cells much more resistant to TGF-β induced cell growth inhibition (Fig.1a, b). These results have been confirmed in another kind of HMEC system-MCF-12A cells (Fig.2a, b). Meanwhile, I found that p21, the key downstream effector responsible for TGF-β induced cell cycle arrest, is downregulated in 10A.14-3-3ζ cells compared to 10A.Vec cells (Fig.3 a, b). Moreover, 14-3-3ζ overexpression also inhibits TGF-β induced p21 gene expression (Fig.3 a, b). I examined whether 14-3-3ζ overexpression inhibits TGF-β induced p15 gene expression or whether it affects TGF-β's inhibition of c-myc gene expression. 14-3-3ζ overexpression inhibits TGF-β induced p15 gene expression as shown in Fig.4a. However, p15 may not be the major downstream executor of TGF-β's cytostatic program in MCF-10A cells because these cells have trace levels of p15 protein expressed. In addition, I found that 14-3-3ζ overexpression does not change TGF-β's inhibition of c-myc dramatically, although 14-3-3ζ overexpression indeed upregulates endogenous c-myc gene expression (Fig.4b).

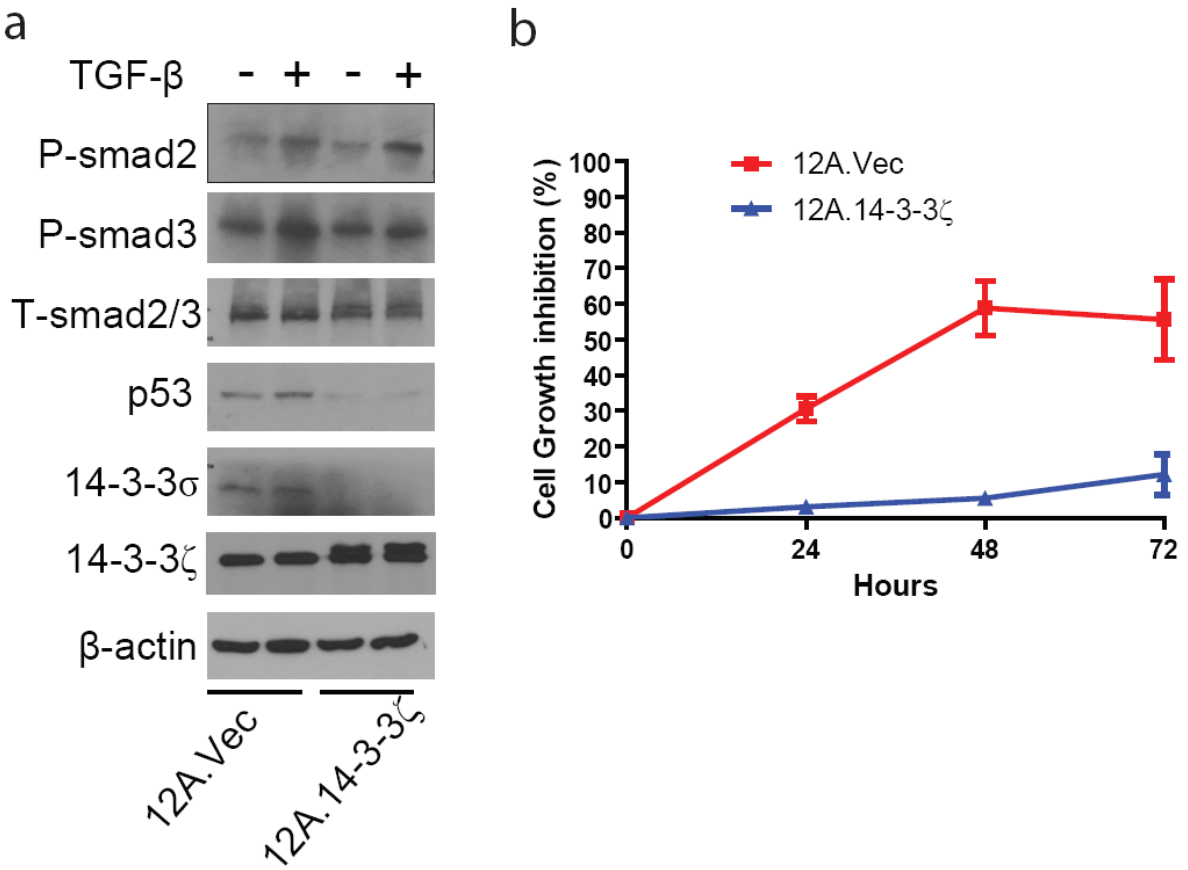

Figure 2. 14-3-3ζ overexpression inhibits TGF-β's cytostatic function in MCF-12A cells. a) Western blot analysis of TGF-β signaling pathway in MCF-12A.Vec and MCF-12A.14-3-3ζ with or without TGF-β treatment for 2 hours. b) MCF-12A.Vec or MCF-12A.14-3-3ζ cells treated with TGF-β (5ng/ml) or vehicle. Cells were counted every 24 hours and plotted as percent inhibition relative to vehicle control.

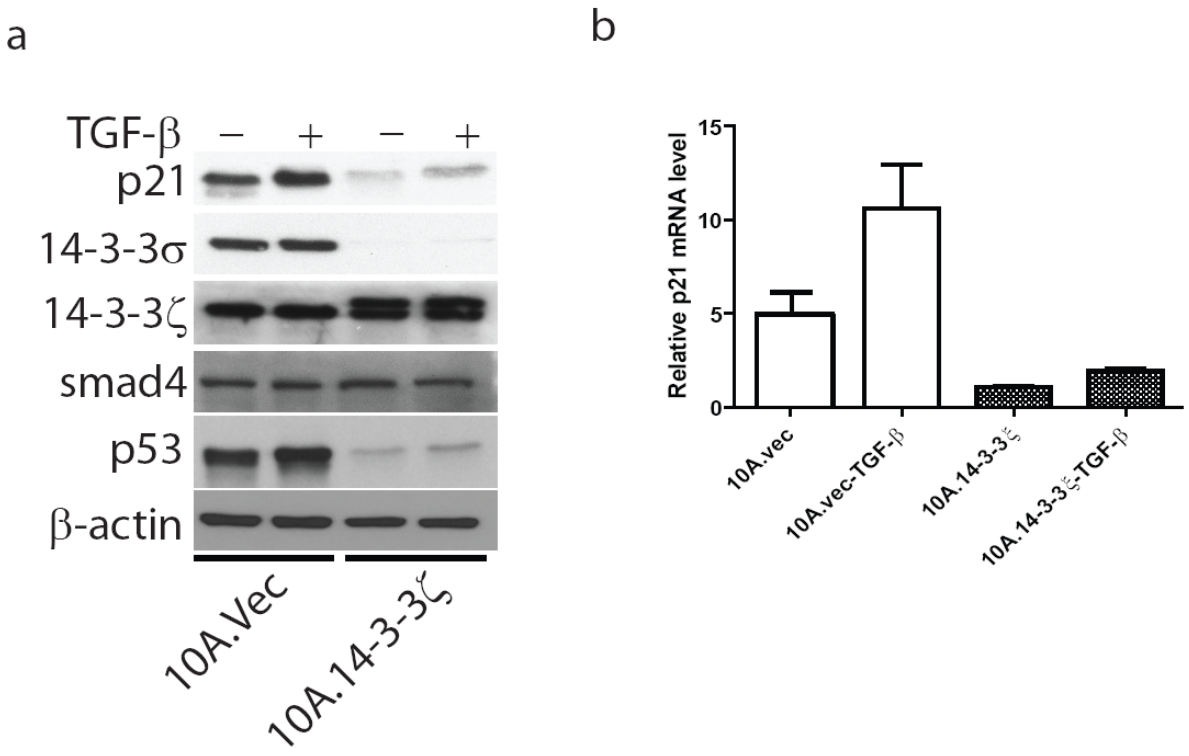

Figure 3. 14-3-3ζ overexpression switches off TGF-β's cytostatic program through inhibiting p21 expression. a) Western blot analysis of MCF-10A.Vec and MCF-10A.14-3-3ζ with or without TGF-β treatment for 2 hours. b) RT-PCR analysis of p21 mRNA level in MCF-10A.Vec or MCF-10A.14-3-3ζ cells treated with TGF-β (5ng/ml) or vehicle for 2 hours. Normalized to GAPDH and relative to 10A.14-3-3ζ cells

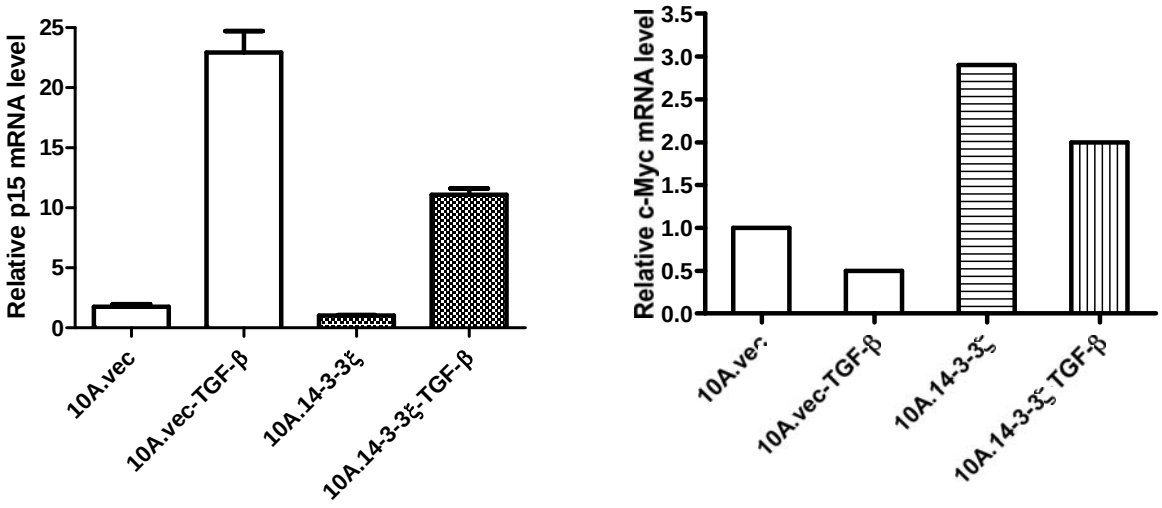

Figure 4. 14-3-3ζ overexpression switches off TGF-β's cytostatic program, but not through p15 or c-myc.
RT-PCR analysis of p21 mRNA level (Left panel) and c-myc mRNA level (right panel) in MCF-10A.Vec or MCF-10A.14-3-3ζ cells treated with TGF-β (5ng/ml) or vehicle for 2 hours. Normalized to GAPDH and relative to 10A.Vec cells.

To further test if p21 is the final executor for TGF-β induced cell proliferation inhibition in MCF-10A cells, I knocked down p21 in MCF-10A cell (Fig.5a) and found that MCF-10A.p21shRNA233 and MCF-10A.p21shRNA535 are resistant to the cell proliferation inhibition function of TGF-β compared to MCF-10A.scramble cells (Fig.5b). Additionally, I found that TGF-β still can induce p21 gene expression partially after p21 knockdown in MCF-10A cell, which suggests that the upstream regulator of p21 expression is still imperturbable (Fig. 6). Taken together, our data indicate that TGF-β induces p21 gene expression to inhibit cell proliferation in non-transformed human mammary epithelial cells, and 14-3-3ζ overexpression inhibits TGF-β's cytostatic program in normal epithelial cells through downregulation of p21.

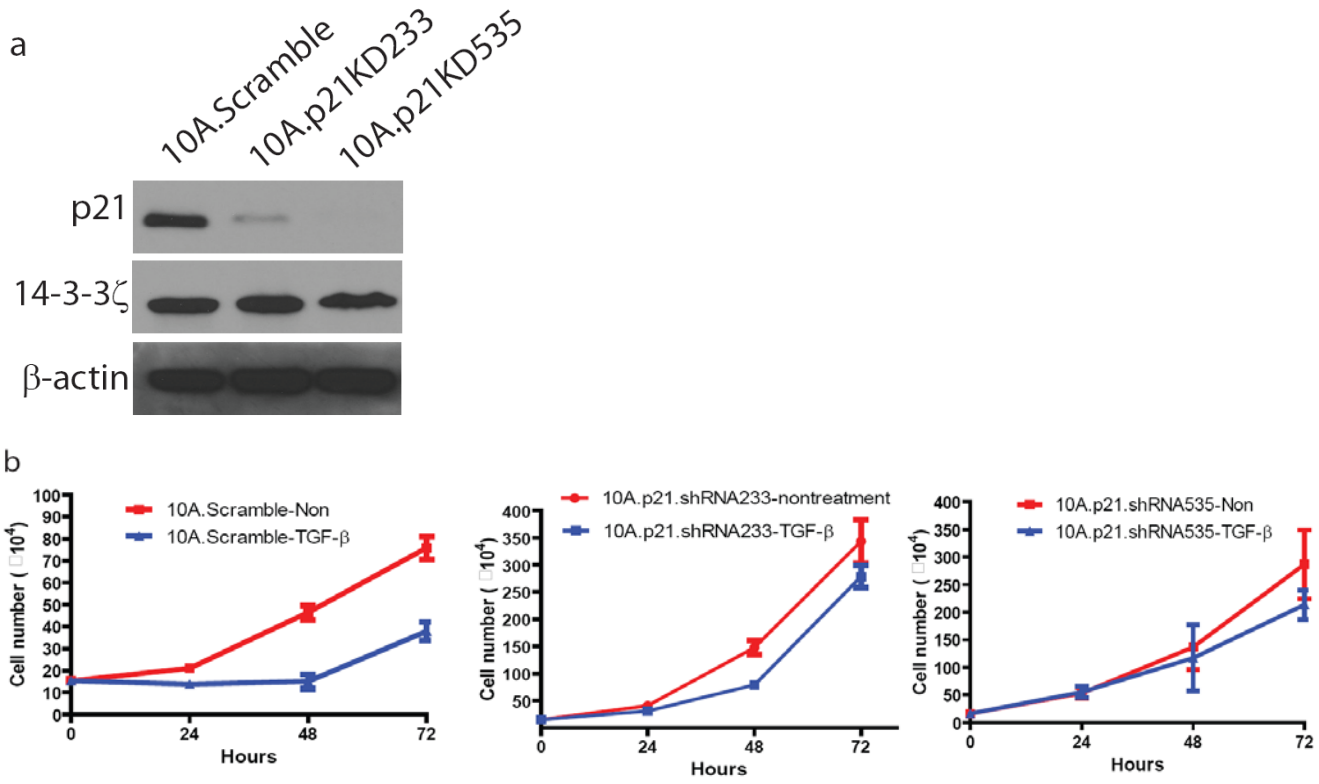

Figure 5. Knockdown of p21 in MCF-10A cells inhibits TGF-β's cytostatic function.
a) Multiple MCF10A stable clones were established with p21 knockdown. Immunoblot analysis of p21 is shown. b) MCF-10A.scramble, MCF-10A.p21shRNA233, and MCF-10A.p21shRNA535 cells treated with TGF-β (5 ng/ml) or vehicle for 24, 48, 72 hours respectively. Cell proliferation was measured by counting cell number with a Levy hemocytometer. Data are presented as the mean ± SD of three independent experiments.

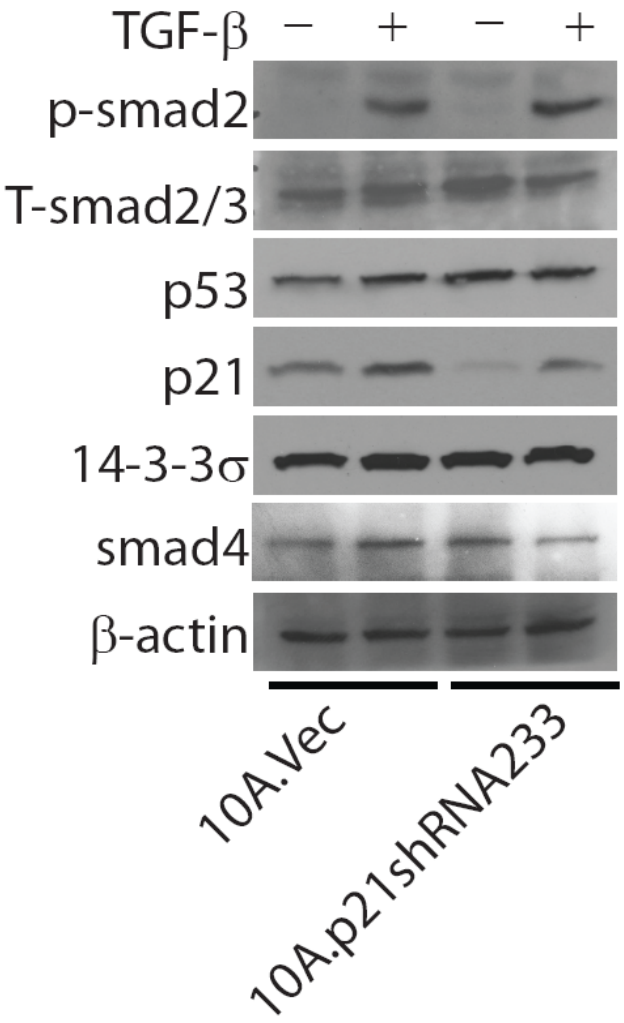

Figure 6. p21 is the final executor of TGF-β's cytostatic program in non-transformed human mammary epithelial cells.
Western blot analysis of TGF-β's cytostatic program in MCF-10A.scramble and MCF-10A.p21shRNA233 cells treated with TGF-β (5ng/ml) or vehicle for 2 hours.

Destabilization of p53 by 14-3-3ζ overexpression suppresses TGF-β induced p21 expression

In mammalian cells, the full transcriptional activation of the CDK inhibitor p21 by TGF-β requires a specific co-transcription activator to co-operate with smad complexes. However, this signaling cascade is cell-context dependent. The forkhead box (Foxo) family of transcription factors especially FOXO3a, has been reported to form complexes with smad3/4 to turn on p21 in response to TGF-β in HaCaT cells. This effect can be negatively regulated by PI3K-Akt activation because Akt directly phosphorylates FOXO3 and forces FOXO3 out of nucleus, thereby preventing it ability to activate p21 gene transcription (38). Moreover, 14-3-3 has been shown to be responsible for sequestering FOXO3 in the cytosol after Akt phosphorylation (49), so we tested whether 14-3-3ζ overexpression blocks the complex formation of FOXO3 and smads. However, we did not find that FOXO3a could form a complex with smads in response to TGF-β stimulation in MCF-10A cells as the previously shown (Fig. 7), this might suggest that in different cell contexts, TGF-β signaling pathway may utilize different co-transcription factors together with smads to turn on p21 expression.

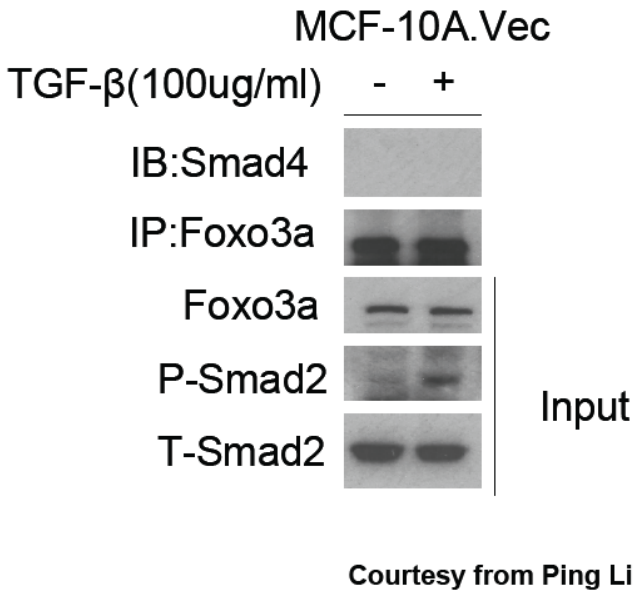

Figure 7. Foxo3a does not form a complex with smad4 in response to TGF-β in MCF-10A cells.

MCF-10A.Vec cells were treated with TGF-β (5ng/ml) or vehicle for 2 hours. Total cell lysates were collected followed by Immunopreciptation with Foxo3a antibody, and immunoblot analysis of smad4 as indicated.

In addition to FOXO3, p53 also has been shown to be required for TGF-β induced p21 expression (50-52), and 14-3-3ζ overexpression can lead to p53 downregulation through activating the PI3K/Akt pathway, which leads to phosphorylation and translocation of the MDM2 E3 ligase, resulting in increased p53 degradation (3). Therefore, we examined whether p53 can form a complex with smads in MCF-10A cells. In the absence of TGF-β stimulation, p53 does not bind to smad2 in MCF-10A.vec cells (Fig. 8). However, in MCF-10A.14-3-3ζ cells, 14-3-3ζ overexpression downregulates p53 (Fig.2 & Fig.3), and thereby downregulates endogenous p21 expression which is important for TGF-β's cytostatic function as indicated previously. After TGF-β treatment, we found that p53 binds to smad2 in MCF-10A cells (Fig 8), but in 10A.ζ cells, TGF-β cannot induce p21 expression due to lack of co-transcription factor p53 (Fig.2 & Fig.3). These data suggests that in human mammary epithelial cells, p53 is the major co-transcription factor required for TGF-β induced p21 expression, and downregulation of p53 by 14-3-3ζ blocks TGF-β's cytostatic program.

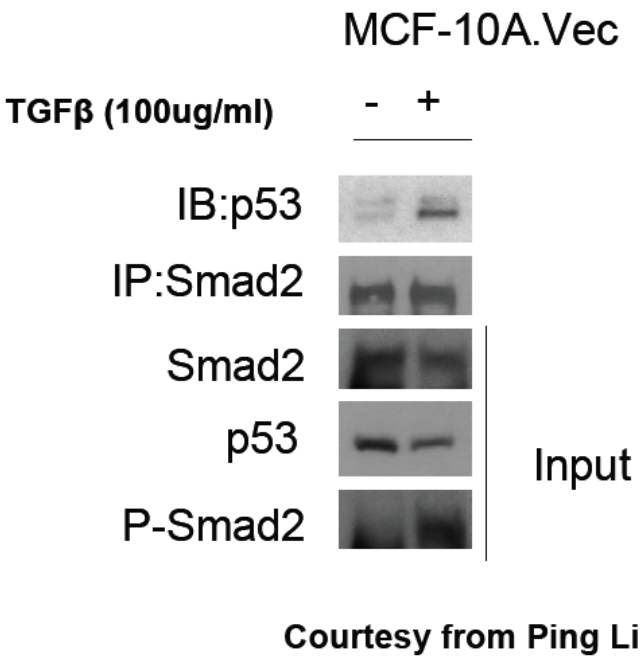

Figure 8. p53 forms a complex with smad2 in response to TGF-β in MCF-10A cells. MCF-10A.Vec treated with TGF-β (5ng/ml) or vehicle for 2 hours. Total cell lysates were collected and immunoprecipitated with smad2 antibody followed by immunobloting analysis of p53 as indicated.

14-3-3σ downregulation by 14-3-3ζ overexpression contributes to destabilization of p53 in non-transformed HMEC cells

Our previous data has shown that p53 downregulation in MCF-10A.14-3-3ζ cells is due to activation of the PI3K/Akt pathway by 14-3-3ζ overexpression, which phosphorylates MDM2 resulting in proteasomal degradation of p53 (3). However, 14-3-3σ, another 14-3-3 family member, has been reported to inhibit Akt activation (53) and stabilize p53 in an opposite fashion (54). In addition, to obtain an unbiased and comprehensive view of 14-3-3ζ-mediated molecular alterations, I performed cDNA microarrays in MCF-10A.14-3-3ζ cells versus MCF-10A.vec control cells grown under 3D culture conditions. Interestingly, I found that 14-3-3σ is downregulated in MCF-10A.14-3-3ζ cells compared to MCF-10A.Vec cells (Fig. 9a). These findings were confirmed by RT-PCR and western blot in both MCF-10A and MCF-12A cells (Fig. 9b, c).

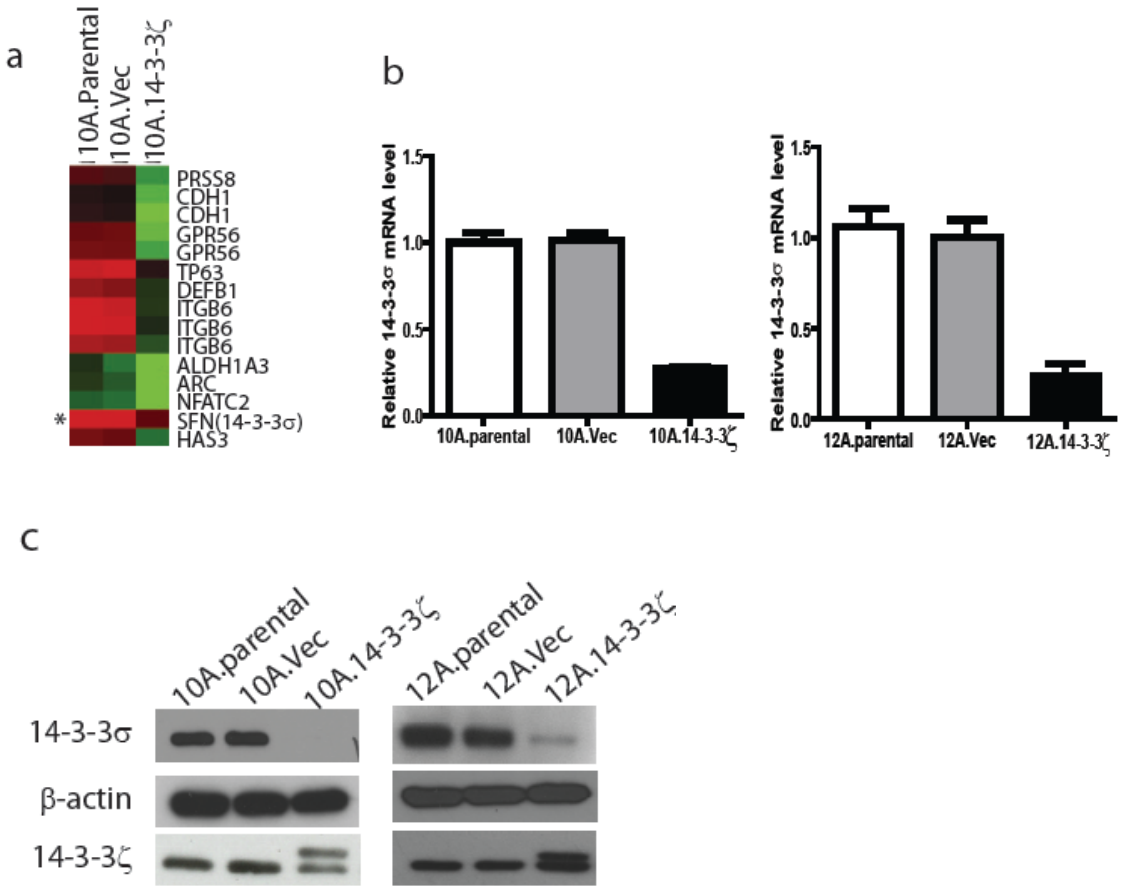

Figure 9. 14-3-3ζ overexpression leads to downregulation of 14-3-3σ via transcriptional inhibition.

a) Gene expression profiling on 10A.parental, 10A.vec and 10A.14-3-3ζ cells using cDNA microarray. Heat map depicts top gene alterations in 10A.14-3-3ζ cells versus 10A.Vec cells. b) RT-PCR analysis of 14-3-3σ mRNA level in 10A.parental, 10A.Vec, and 10A.14-3-3ζ cells (left panel). RT-PCR analysis of 14-3-3σ mRNA level in 12A.parental, 12A.Vec and 12A.14-3-3ζ cells was also performed (right panel). c) Western blot analysis of 14-3-3σ and 14-3-3ζ protein level in MCF-10A sublines and MCF-12A sublines. β-actin was used as a loading control.

To test if 14-3-3σ downregulation by 14-3-3ζ overexpression contributes to destabilization of p53 in non-transformed HMEC cells, I knocked down 14-3-3σ in 10A cells and found that phosphorylation of Akt increased and p53 was downregulated in MCF-10A.14-3-3σshRNA128 cells compared to MCF-10A.Scramble cells (Fig. 10a). Consistent with this, p53 was recovered and Akt activation was inhibited after 14-3-3σ was rescued in MCF-10A.14-3-3ζ cells (Fig. 11a). To further investigate if downregulation of 14-3-3σ is critical for 14-3-3ζ blocking the TGF-β induced cytostatic program, I treated MCF-10A.14-3-3σshRNA128 cells with TGF-β and found that 14-3-3σ knockdown renders MCF-10A cells resistant to TGF-β-mediated cell growth inhibition (Fig.10b, c), and inhibits TGF-β induced p21 expression (Fig. 10a). Additionally, rescuing 14-3-3σ in MCF-10A.14-3-3ζ cells renders MCF-10A.14-3-3ζ cells sensitive to TGF-β treatment (Fig.11b), and also recovers TGF-β induced p21 gene expression in MCF-10A.14-3-3ζ.14-3-3σ cells (Fig.12). Taken together, these data suggest that 14-3-3ζ and 14-3-3σ play an opposite role in mediating TGF-β induced p21 gene expression and cell proliferation inhibition. Importantly, these data may support the hypothesis that 14-3-3ζ-mediated downregulation of 14-3-3σ leads to destabilization of p53 in non-transformed human mammary epithelial cells and switches off TGF-β's tumor suppressor function in the early stage of breast cancer development to contribute to the progression of breast cancer.

a

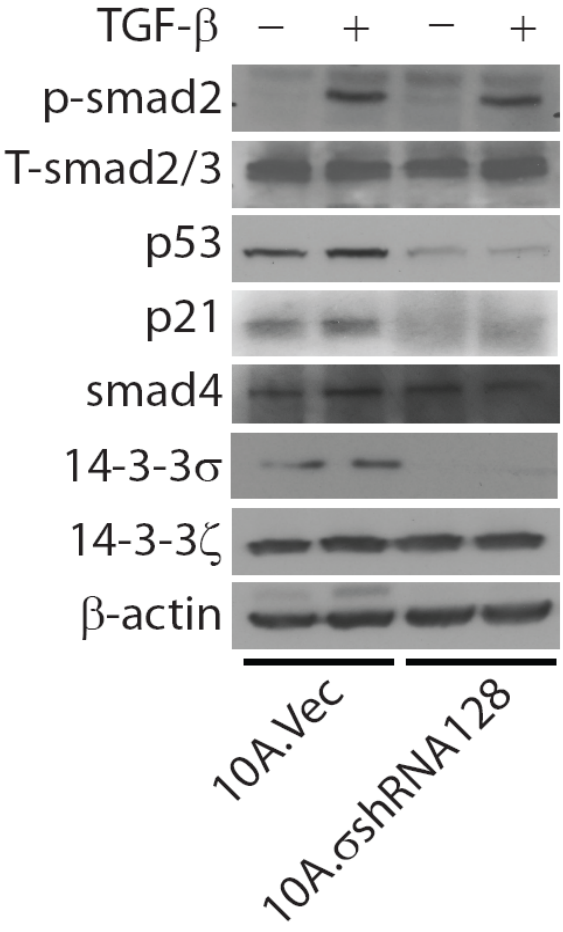
TGF-β − + − +
p-smad2
T-smad2/3
p53
p21
smad4
14-3-3σ
14-3-3ζ
β-actin
10A.Vec
10A.σshRNA128

b

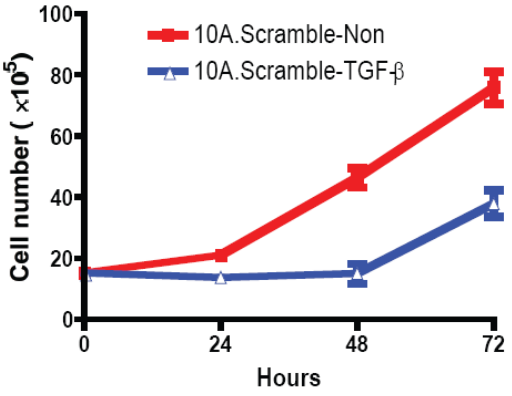
10A.Scramble-Non
10A.Scramble-TGF-β
Cell number (×10^5)
Hours
0
24
48
72
20
40
60
80
100

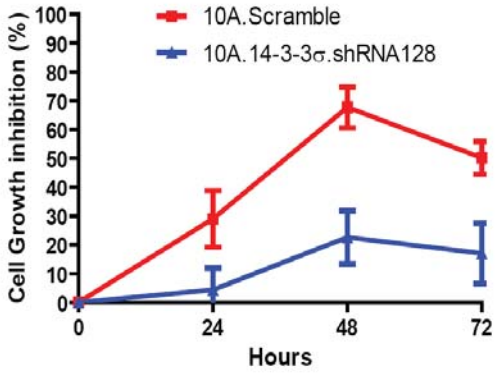
10A.Scramble
10A.14-3-3σ.shRNA128
Cell Growth inhibition (%)
Hours
0
10
20
30
40
50
60
70
80
90
100
24
48
72

C

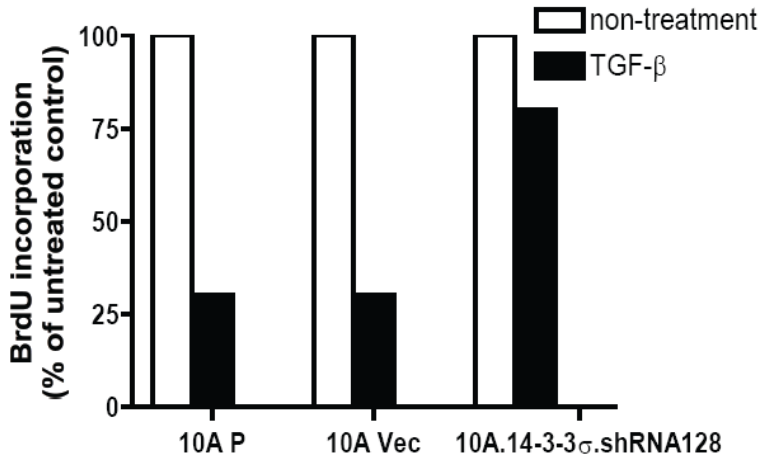

Figure 10. knockdown of 14-3-3σ inhibits TGF-β's cytostatic function.
a) After knockdown of 14-3-3σ in MCF-10A cells, MCF-10A.scramble and MCF-10A.σsh128 cells treated with TGF-β (5ng/ml) or vehicle for 2 hours followed by Western blot analysis of TGF-β's cytostatic program in 10A.scramble and 10A.σsh128 cells. b) MCF-10A.scramble or MCF-10A.σsh128 cells were treated with TGF-β (5ng/ml) or vehicle. Cells were counted every 24 hours and plotted as percent inhibition relative to vehicle control. c) BrdU incorporation assay on 10A.scramble and 10A.σsh128 cells treated with TGF-β (5ng/ml) or vehicle for 72 hours. The percentage of cell proliferation was calculated after 72 hours treatment and normalized to the group without treatment.

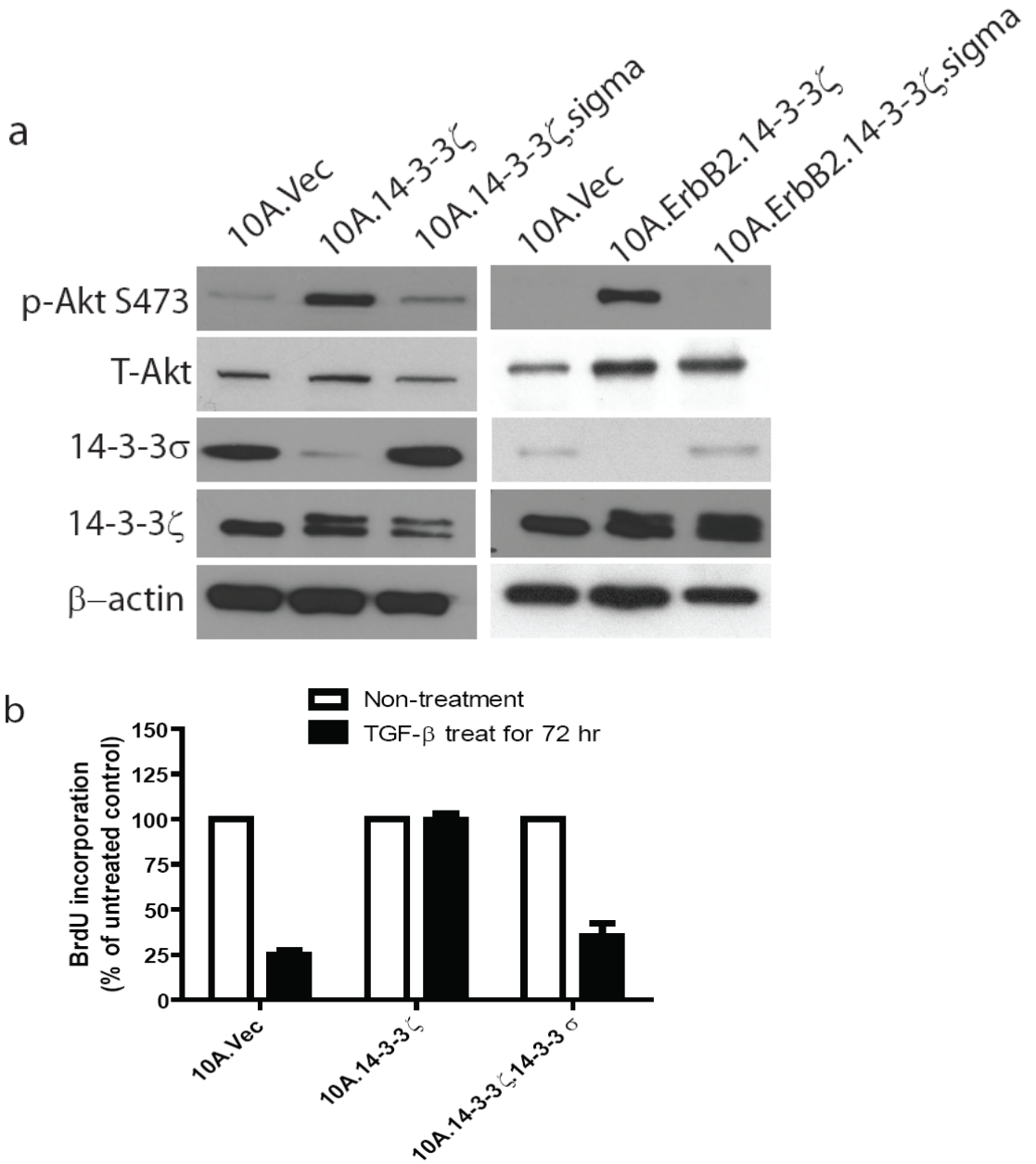

Figure 11. 14-3-3σ downregulation contributes to PI3K-Akt activation and p53 destabilization induced by 14-3-3ζ overexpression, thereby contributes to the inhibition of TGF-β's cytostatic program by 14-3-3ζ overexpression.

a) 14-3-3σ expression was rescued in 10A.14-3-3ζ and 10A.ErbB2.14-3-3ζ cells and western blot analysis of p-Akt, T-Akt, 14-3-3σ, 14-3-3ζ in 10A.vec, 10A.14-3-3ζ, 10A.14-3-3ζ.sigma cells (Left panel) and 10A.ErbB2.14-3-3ζ and 10A.ErbB2.14-3-3ζ.sigma cells (right panel) was performed. β-actin was used as a loading control. b) BrdU incorporation assay in 10A.vec, 10A.14-3-3ζ, 10A.14-3-3ζ.sigma cells treated with TGF-β (5ng/ml) or vehicle for 72 hours.

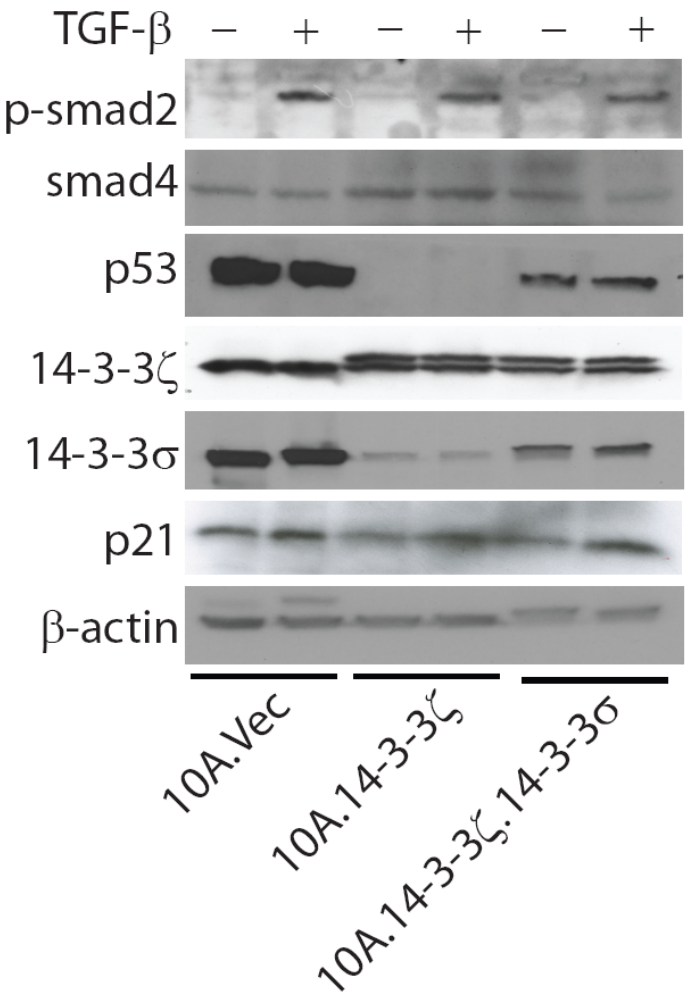

Figure 12. Rescue of 14-3-3σ in 10A.14-3-3ζ cells recovers the cytostatic function of TGF-β.
After rescue of 14-3-3σ in MCF-10A.14-3-3ζ cells, the MCF-10A sublines were treated with TGF-β (5ng/ml) or vehicle for 2 hours as indicated followed by Western blot analysis of TGF-β's cytostatic program in MCF-10A sublines.

14-3-3ζ overexpression downregulates 14-3-3σ in the early stage of breast cancer development though sequestering YAP1 transcription factor in the cytosol

I have already found 14-3-3σ (SFN) was significantly downregulated in 10A.14-3-3ζ cells compared to 10A.vec cells (Fig. 9a), and confirmed cDNA microarray data at both mRNA and protein level by performing RT-PCR and western blot (Fig. 9b, c). To test if this is a cell specific phenotype or retrovirus effect, I established another 14-3-3ζ overexpressing HMEC cell line in MCF-12A cells by transduction with a lentiviral vector containing 14-3-3ζ gene with an N-terminal HA-tag. Consistent with my previous findings in MCF-10A cells, I found a downregulation of 14-3-3σ expression following 14-3-3ζ overexpression (Fig. 9b, c). Additionally, I found that 14-3-3σ is upregulated at both the mRNA and protein level in 14-3-3ζ-/- Mouse embryonic fibroblast (MEF) cells compare to 14-3-3ζ+/+ and 14-3-3ζ+/- MEF cells (Fig. 13). Moreover, 14-3-3σ is downregulated by 14-3-3ζ overexpression in the mammary gland tissues at lactation day 20 of WAP-HA-14-3-3ζ mouse compared to wild type mice (Data not shown). To investigate if this regulation is prevalent in breast cancer, I also determined 14-3-3ζ and 14-3-3σ protein level in a panel of cell lines including non-transformed HMEC cells and malignant breast cancer cells, and found out that 14-3-3ζ is generally highly expressed in breast cancer cells compared to non-transformed HMEC cells; however, the expression of 14-3-3σ is lost in breast cancer cells compared to non-transformed HMEC cells (Fig. 14). These data suggest that downregulation of 14-3-3σ by 14-3-3ζ overexpression is a prevalent phenomenon that exists in breast cancer cells, and this regulation may contribute to the dynamic balance of 14-3-3 family members in breast cancer development and dimorphic function of these two well-known members.

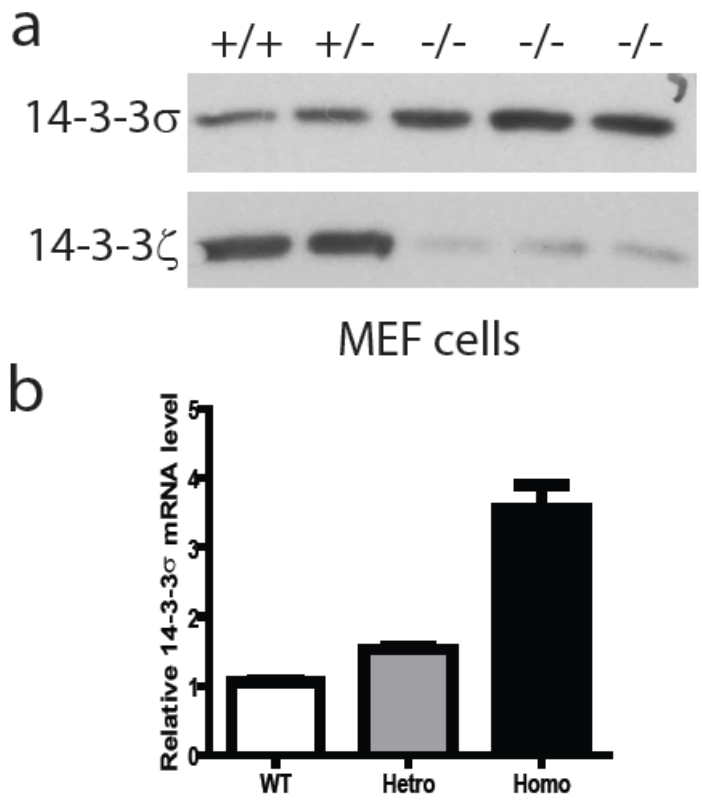

Figure 13. 14-3-3σ is upregulated in 14-3-3ζ knockout mice.
a) Western blot analysis of 14-3-3σ protein level in MEF cells from wild type, 14-3-3ζ+/-, 14-3-3ζ-/- mice. b) RT-PCR analysis of 14-3-3σ protein level in MEF cells from wild type, 14-3-3ζ+/-, 14-3-3ζ-/- mice.

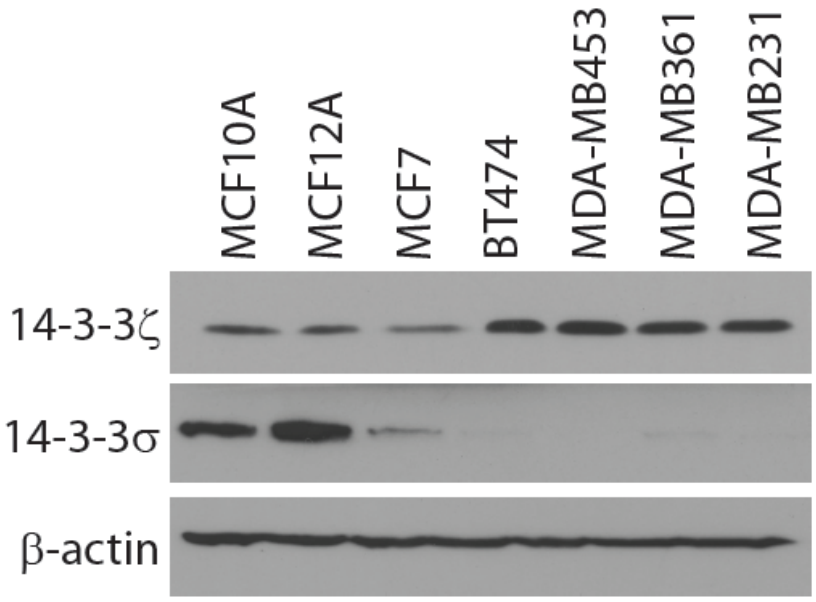

Figure 14. 14-3-3ζ and 14-3-3σ are inversely correlated in a panel of non-transformed HMEC cells and breast cancer cells.
Western blot analysis of 14-3-3σ and 14-3-3ζ protein level in a panel of non-transformed HMEC cells and breast cancer cells.

Since I found that downregulation of 14-3-3σ by 14-3-3ζ overexpression is at the mRNA level, I investigated the mechanism by which 14-3-3ζ regulates the mRNA of 14-3-3σ. The transcription and expression of 14-3-3σ can be regulated in multiple ways. For example, P53 can induce 14-3-3σ in response to ionizing radiation and DNA damage (16). p53 is dephosphorylated and activated following cellular DNA damage, and it then binds to the promoter region of 14-3-3σ, and lead to increased transcription of 14-3-3σ and G2/M arrest (16, 55). In basal/progenitor cell, 14-3-3σ expression may be repressed by ΔNp63, a dominant negative isoform which can suppress both p53 and TAp63 transactivation (21, 23). To test if downregulation of 14-3-3σ in 10A.14-3-3ζ cell is due to increased proteasomal degradation of transcitption factor-p53, I rescued p53 in 10A.14-3-3ζ cells by treating 10A.14-3-3ζ cells with MG132, but I did not find 14-3-3σ was recovered in 10.14-3-3ζ cell along the time course (Fig. 15). Although p53 and ΔNp63 have been reported to be the major regulator of 14-3-3σ expression in cell lines, no association between 14-3-3σ expression and p53 mutations or increased level of ΔNp63 was seen in human tissue, suggesting that the constitutive expression of 14-3-3σ may be dependent on factors other than p53(32), and p53 probably transactives 14-3-3σ expression only in response to DNA damage stimuli. In addition, 14-3-3σ also can be regulated by estrogen-induced zinc finger protein (EFP). Through interacting with EFP, 14-3-3σ gets ubiquitinylated and quickly degraded by EFP in breast epithelial cells (24). Recently, Gene silencing of 14-3-3σ, mainly modulated by CpG methylation in the promoter region, has been reported in several types of solid tumor, including prostate, lung, breast, skin cancer, and also in hematologic malignancies (25-28, 31). To test this, I determined the promoter methylation level of 14-3-3σ in 10A.14-3-3ζ cells by performing bisulfite genomic sequencing (Fig. 16a). There was

no difference in the methylation level in 10A.14-3-3ζ cells compared to 10A.Vec cells. Additionally, 14-3-3σ protein could not be recovered after treating 10A.14-3-3ζ cells with DNA methylation inhibitor 5-Aza-2'-deoxycytidine (Fig. 16b). Collectively, these data suggest that 14-3-3σ mRNA level downregulation by 14-3-3ζ is neither due to decrease of p53 nor due to promoter methylation.

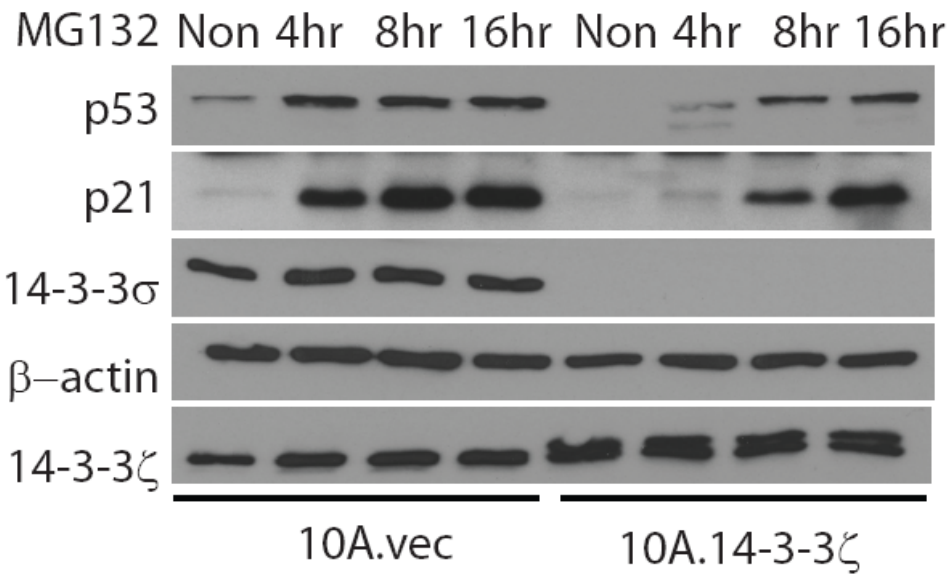

Figure 15. 14-3-3σ downregulation is independent of p53 regulation in 10A cells.
10A.vec and 10A.14-3-3ζ cells were treated with 10μM MG132 or DMSO as previously described, and cell lysates were collected at 4, 8, or 16 hours followed by western blot analysis of p53, p21, 14-3-3σ and 14-3-3ζ protein level. β-actin was used as a loading control.

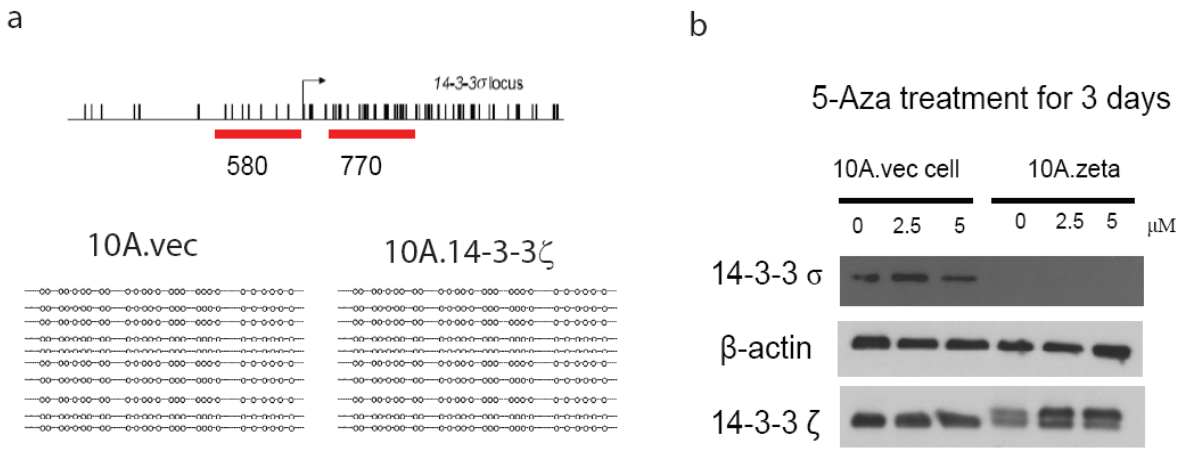

Figure 16. 14-3-3σ downregulation is not due to promoter methylation.
a) Bisulfite Genomic Sequencing analysis of 14-3-3σ promoter CpG islands in 10A.Vec and 10A.14-3-3ζ cells. The CpG island is depicted on the top left panel, and each vertical bar denotes a single CpG. The transcription start site is indicated as an arrow. Two pairs of primers are indicated as red bars which are located both upstream and downstream of the transcription start site. Ten single clones are represented for each sample. Black and white circles represent methylated and unmethylated CpG, respectively. Each circle represents one CpG site. b) 10A.vec and 10A.14-3-3ζ cells were treated with 5-Aza-2'-deoxycytidine at concentrations of 0, 2.5, or 5μM, and cell lysates were collected three days later and followed by western blot analysis of 14-3-3σ and 14-3-3ζ protein level.

In addition, I found that 14-3-3σ mRNA decrease in MCF-10A.14-3-3ζ cells is not due to mRNA stability decrease as shown by 14-3-3σ mRNA decay assay (Fig. 17). To investigate the transcription repression mechanism mediated by 14-3-3ζ, I created a series of 5' deletion mutation constructs of the 14-3-3σ promoter (Fig. 18a) to find the specific promoter region responsible for its transcriptional repression by 14-3-3ζ. Interestingly, I found a specific promoter region of 181bp (from -922bp to -741bp) to be the transcription factor binding region responsible for transcription activation of 14-3-3σ (not including p53 binding sites, Fig. 18b). After analysis of this specific promoter region by online software (Targetscan and TESS, http://www.cbil.upenn.edu/), I found that there are several transcription factor binding sites within this region (Fig. 18a). Therefore, I mutated these binding sites individually and found that one of these sites (M2) is responsible for transcription activation of 14-3-3σ, which is a binding site for the transcription co-activator YAP1 (Fig. 18c). To test if YAP1 is the transcription activator for 14-3-3σ, I knocked down YAP1 in 10A cells, and found that 14-3-3σ is downregulated at both the mRNA and protein level(Fig. 19a, b). In summary, I have found that YAP1 is a novel transcription activator for 14-3-3σ in HMEC cells.

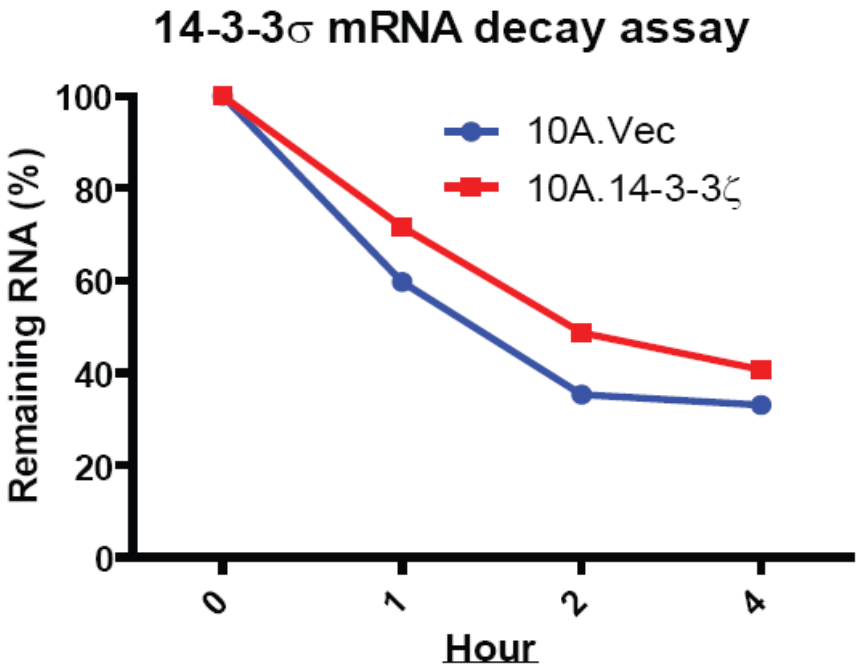

Figure 17. 14-3-3σ downregulation is not due to reduced RNA stability in 10A.14-3-3ζ cells.
10A.vec and 10A.14-3-3ζ cells were treated with the transcription inhibitor Antinomycin D at concentration of 5 μg/ml, and total mRNA was collected at 0, 1, 2, and 4 hours. RNA decay curve shows the remaining 14-3-3σ mRNA level. The value at time 0 was taken as 100%.

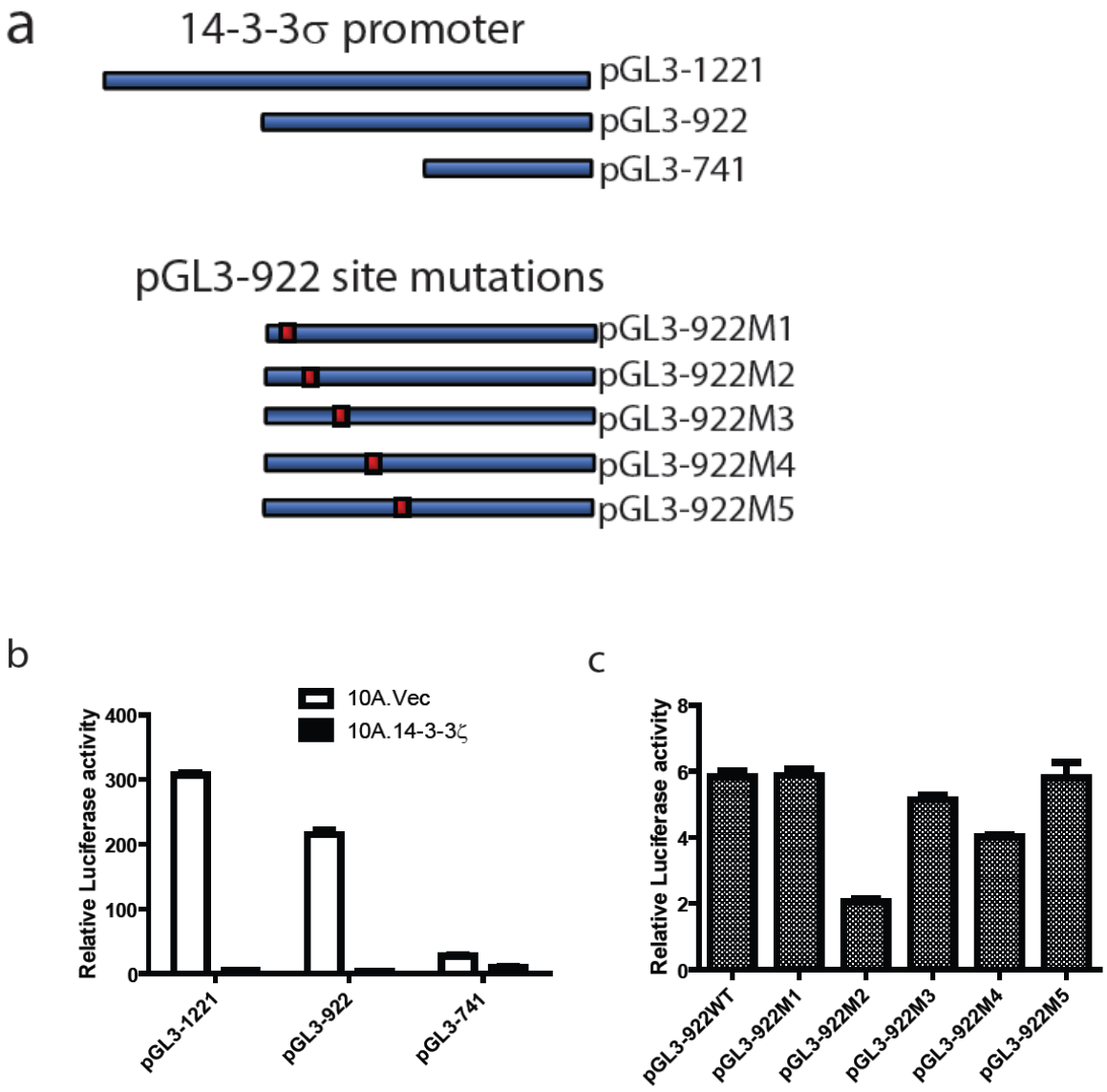

Figure 18. YAP-1 is the transcription factor for 14-3-3σ in 10A cells.
a) The top panel shows a schematic representation of the luciferase reporter gene driven by sequential deletion of the 14-3-3σ promoter. The bottom panel shows a schematic representation of the luciferase reporter gene driven by specific transcription factor binding site mutations in the 14-3-3σ promoter (922bp). b) Relative luciferase activity of pGL3-1221, pGL3-922, and pGL3-741 in MCF-10A.Vec and MCF-10A.14-3-3ζ cells. c) Relative luciferase activity of different site mutations of pGL3.14-3-3σ.922 in MCF-10A.Vec cells. pRL.TK plasmid was co-transfected and used as a transfection efficiency control. Relative luciferase activity was determined 48 hr porst-transfection. Error bars indicate SEM.

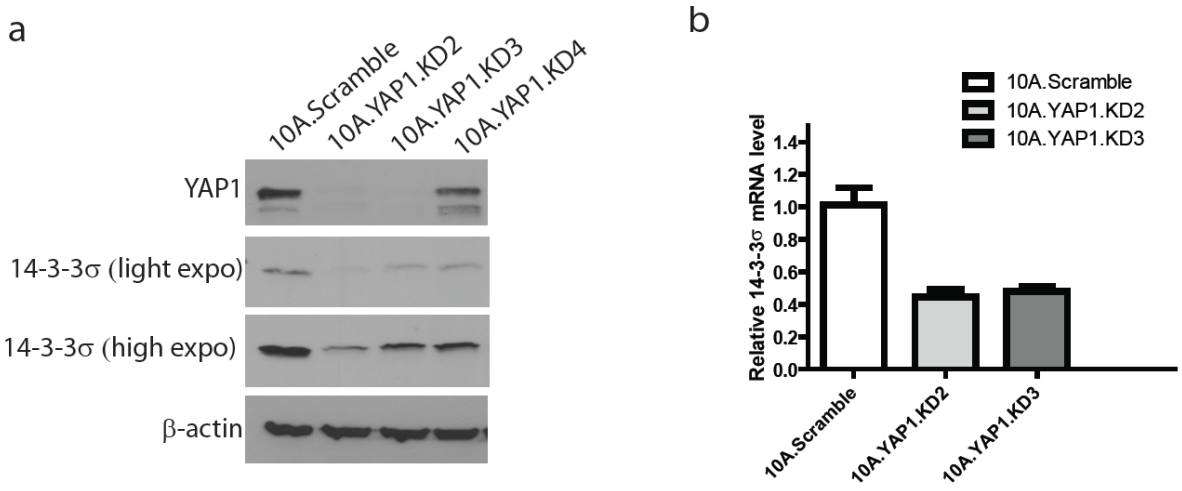

Figure 19. Knockdown of YAP1 leads to downregulation of 14-3-3σ in 10A cells.
Multiple stable clones expressing YAP1 shRNA were established, and most experiments were repeated with different clones to rule out shRNA clonal effects. a) Western blot analysis of 3 sublines for the indicated proteins is shown. b) qRT-PCR analysis of two representative sublines measuring 14-3-3σ mRNA level.

Previous studies discovered that 14-3-3 can bind to YAP1 and retain it in the cytoplasm, and therefore inhibits YAP1 transcription activity (56). Their results combined with my data suggest that 14-3-3ζ may bind to YAP1 and block its shuttling from cytoplasm to nucleus to transactivate 14-3-3σ. To test this hypothesis, I performed an immunoprecipitation assay using anti-HA antibody to pull down 14-3-3ζ and found that 14-3-3ζ binds to phosphorylated YAP1 (Fig. 20) and sequesters YAP1 outside of the nucleus (Fig. 21) in 10A.14-3-3ζ cells. Taken together, our data suggest 14-3-3ζ overexpression downregulates 14-3-3σ in HMEC cells through sequestering YAP1 in the cytoplasm.

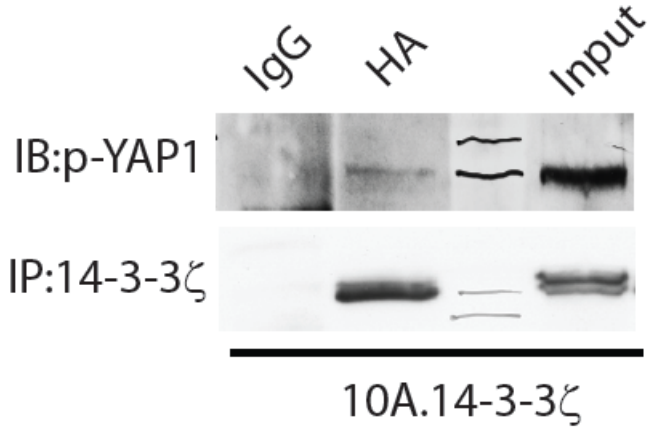

Figure 20. 14-3-3ζ binds to p-YAP-1 in 10A.14-3-3ζ cells.
10A.14-3-3ζ cell lysates were immunoprecipitated by anti-HA antibody, followed by immunoblot analysis of p-YAP1.

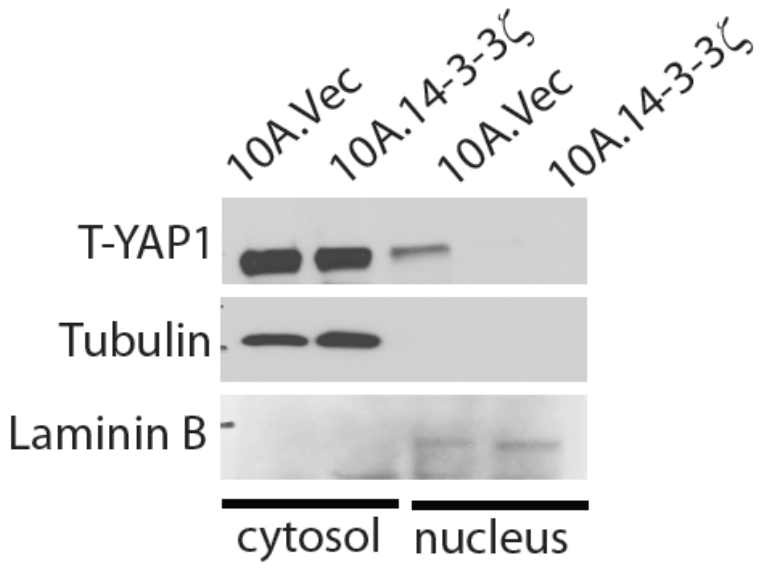

Figure 21. 14-3-3ζ overexpression retains YAP-1 in the cytosol of 10A cells.
MCF-10A.Vec and MCF-10A.14-3-3ζ cells were lysed for cell fractionation followed by western blotting. Lamin B and tubulin were used as markers for the nucleus and the cytoplasm, respectively.

14-3-3ζ overexpression promotes TGF-β induced bone metastatic colonization through activating PTHrP expression

In our previous study, we found that 14-3-3ζ overexpression is critical for TGF-β induced EMT program (19). However, the direct link between 14-3-3ζ overexpression and TGF-β induced breast cancer metastasis is still unknown. Bone is one of the metastatic sites for breast cancer, and bone metastasis is characterized by debilitating bone fractures, severe pain, nerve compression, and hypercalcemia (57). The development and outgrowth of these secondary lesions depends on the intricate cellular and molecular interactions between breast tumor cells and stromal cells of the bone microenvironment(58). One of the abundant cytokines secreted in the bone microenvironment is TGF-β, and it is well known that TGF-β plays an important role in breast cancer bone metastasis (59).

To test whether 14-3-3ζ overexpression in breast cancer cells is essential for TGF-β mediated bone metastasis, I knocked down 14-3-3ζ in MDA-MB-231 cells, which have significantly higher 14-3-3ζ expression compared to non-transformed HMEC cells (MCF-10A) (Fig. 14& 22), and tested their migration ability by performing wound healing assays and transwell migration assays, I found that knocking down 14-3-3ζ in MDA231 cells can dramatically impair TGF-β (5 μg/ml) induced cancer cell migration (Fig. 23). Additionally, 14-3-3ζ knockdown also inhibited MDA231 cells invasion ability under TGF-β stimulation and also without stimulation (Figure not shown). Since TGF-β is the key player in the "vicious cycle" of bone metastasis (60), I sought to determine whether knocking down 14-3-3ζ in MDA231 cells impairs the crosstalk of tumor cells with the bone microenviroment. A panel of MDA231 sublines was co-cultured with osteoblasts (MC3T3) and osteoclasts (RAW264.7) cells *in vitro* under the stimulation of TGF-β or no treatment to investigate the

effect of 14-3-3ζ on the TGF-β-mediated vicious cycle. The results showed a 3-fold increase in the number of MDA231.14-3-3ζ KD tumor cells compared to scramble control when treated with TGF-β after normalization to the counts without coculture (Fig. 24a, b) in the co-culture system with MC3T3 osteoblast cells. However, without TGF-β stimulation, there is no significant difference between 14-3-3ζ knockdown cells and control cells (Fig. 24a, b). Interestingly, I also found that knockdown of 14-3-3ζ in MDA231 cells does not change the proliferation of cancer cells in response to TGF-β in the non-coculture system (Fig. 25). This suggests that knockdown of 14-3-3ζ itself cannot affect proliferation ability when co-cultured with osteoblast cells, but rather loss of 14-3-3ζ inhibits TGF-β mediated tumor cell growth and interaction with osteoblast cells. In addition, I also tested the role of 14-3-3ζ in TGF-β-mediated tumor cell interaction with osteoclast cells by directly coculturing tumor cells with pre-osteoclast RAW264.7 cells. Strikingly, co-culture of MDA231.14-3-3ζ KD cells showed a dramatic decrease in TRAP+ osteoclasts relative to controls (Fig. 26). Collectively, these findings reveal that 14-3-3ζ overexpression in breast cancer cells promotes TGF-β-induced cancer cell proliferation in the bone microenvironment and activates osteoclast maturation and differentiation, thereby contributing to TGF-β-induced osteolytic effect.

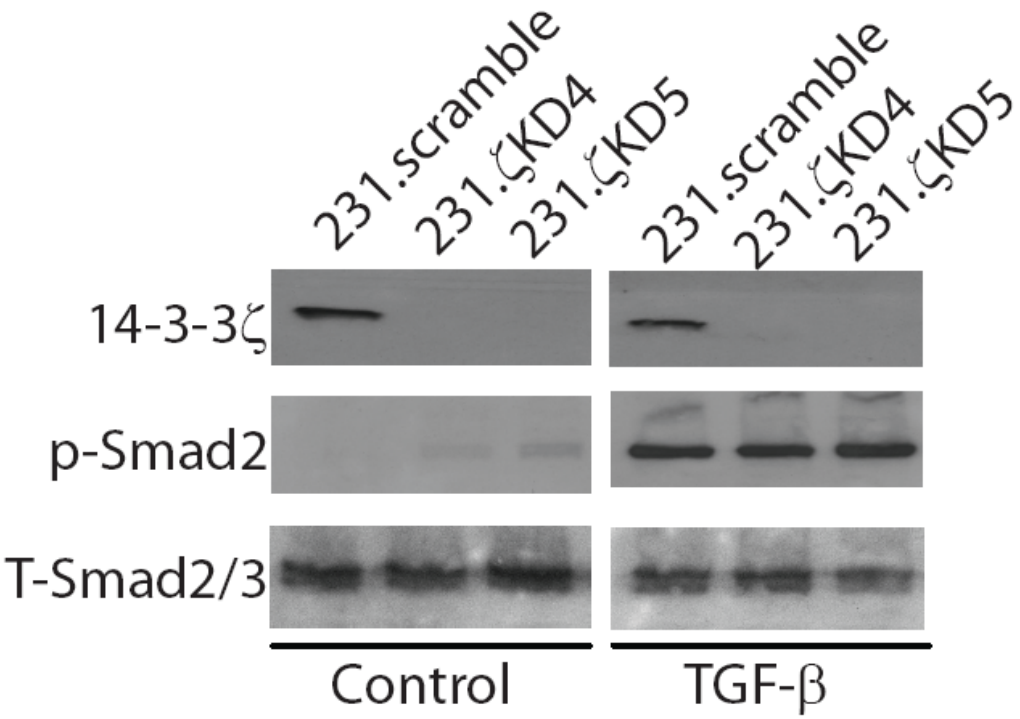

Figure 22. Knockdown of 14-3-3ζ in MDA-MB231 cells.
After 14-3-3ζ knockdown in MDA-MB231 cells, 231.scramble, 231.ζKD4, and 231.ζKD5 cells were treated with TGF-β or vehicle at concentration of 5 μM, and cell lysate were collected at two hours followed by western blot analysis of 14-3-3ζ, p-smad2, and T-smad2/3 protein level. Phosphorylated-smad2 (p-smad2) indicates activation of the TGF-β pathway and T-smad2/3 serves as a loading control.

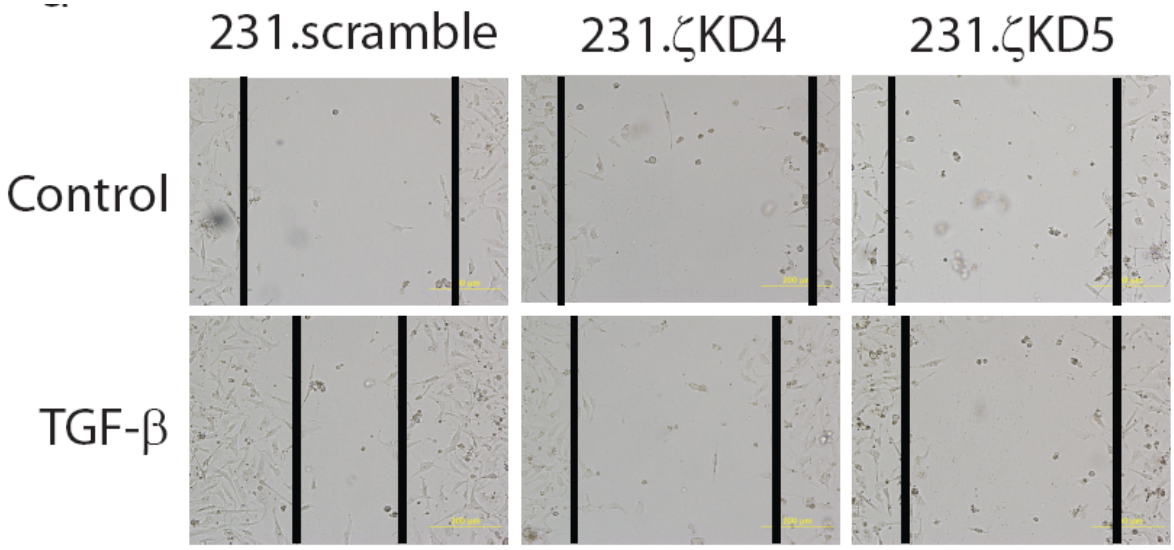

Figure 23. Knockdown of 14-3-3ζ in MDA231 cells inhibits cancer cell migration in response to TGF-β.
Wound healing assay of the indicated MDA231 sublines with treatment of TGF-β (5ng/ml) or vehicle. Wound closures were photographed at 6 hours after wounding. The scale bar represents 200μm.

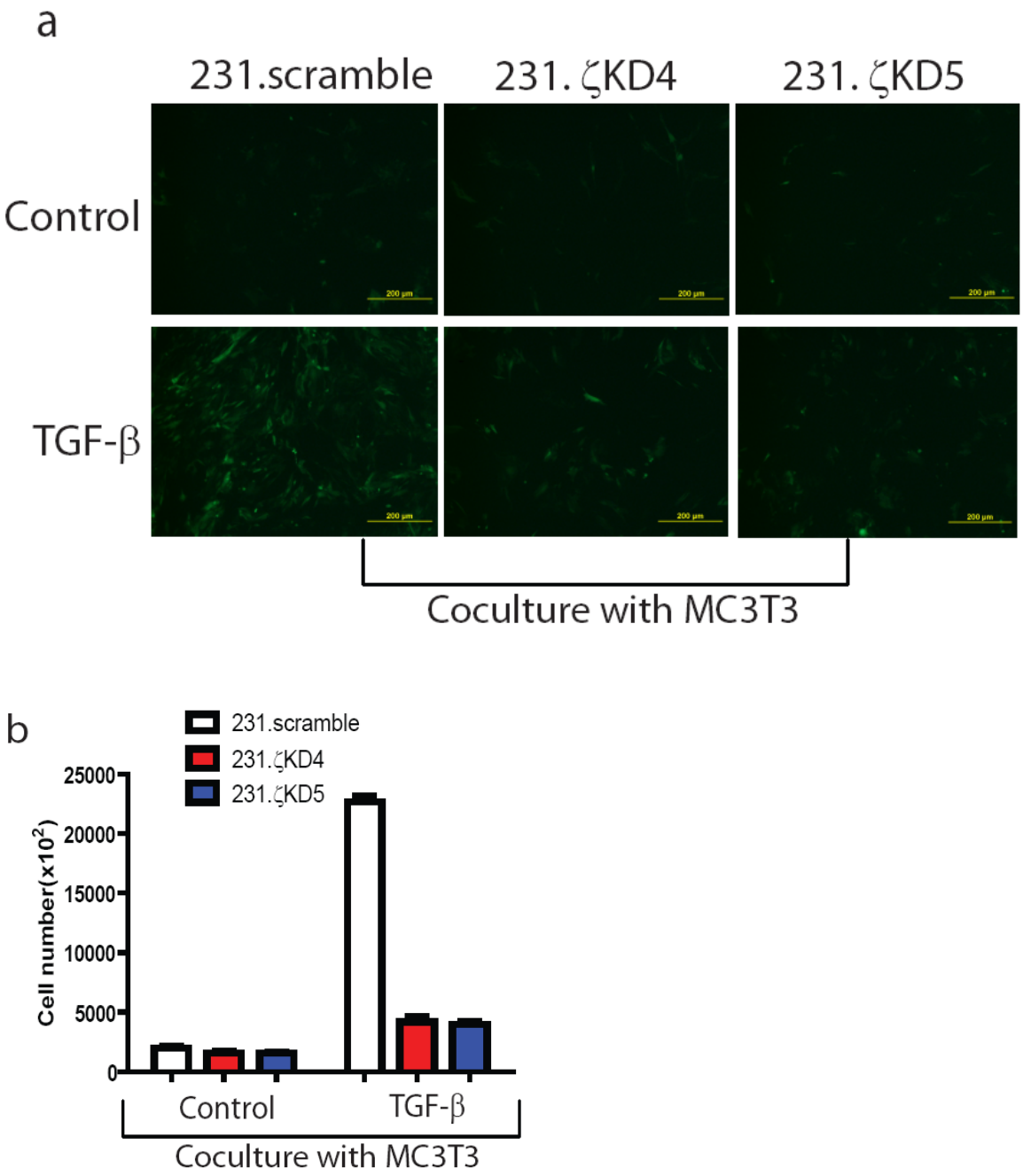

Figure 24. Knockdown of 14-3-3ζ in MDA231 cells inhibits cancer cell proliferation in the co-culture system with MC-3T3 osteoblast cells.
231.scramble, 231.ζKD4, and 231.ζKD5 cells were co-cultured with MC-3T3 osteoblasts cells. In the co-culture system cells were treated with TGF-β at concentration of 5 ng/ml or vehicle, **a)** Representative images of coculture from each experimental group. Scale bar, 200 μm. **b)** Quantification of tumor cells from co-cultures with MC3T3 from each experimental group.

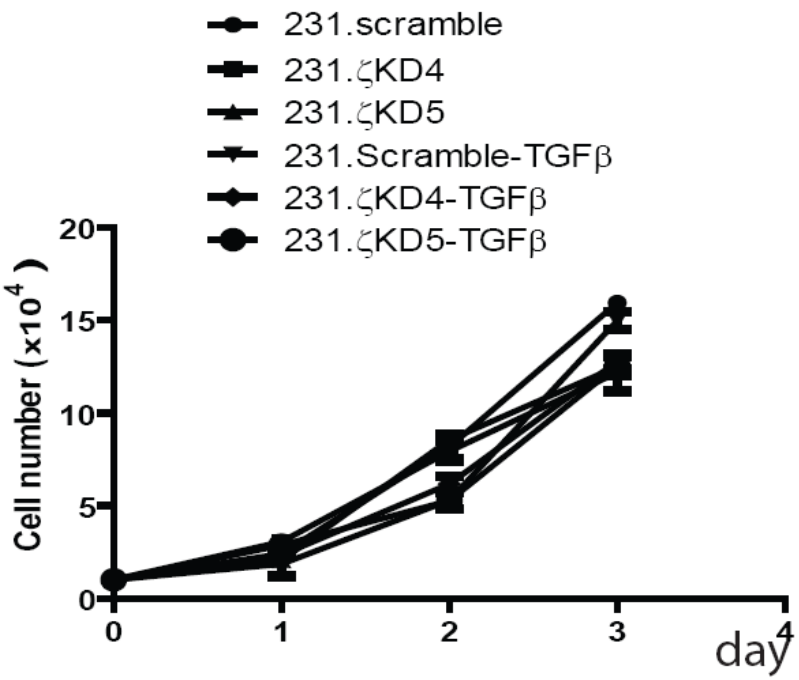

Figure 25. Knockdown of 14-3-3ζ in MDA231 cells does not change cancer cell proliferation in response to TGF-β.
Equal numbers of MDA231 sublines were seeded and treated with TGF-β (5 ng/ml) or vehicle, and cell proliferation was measured by counting cell number with a Levy hemacytometer. Data are presented as the mean ± SD of three independent experiments.

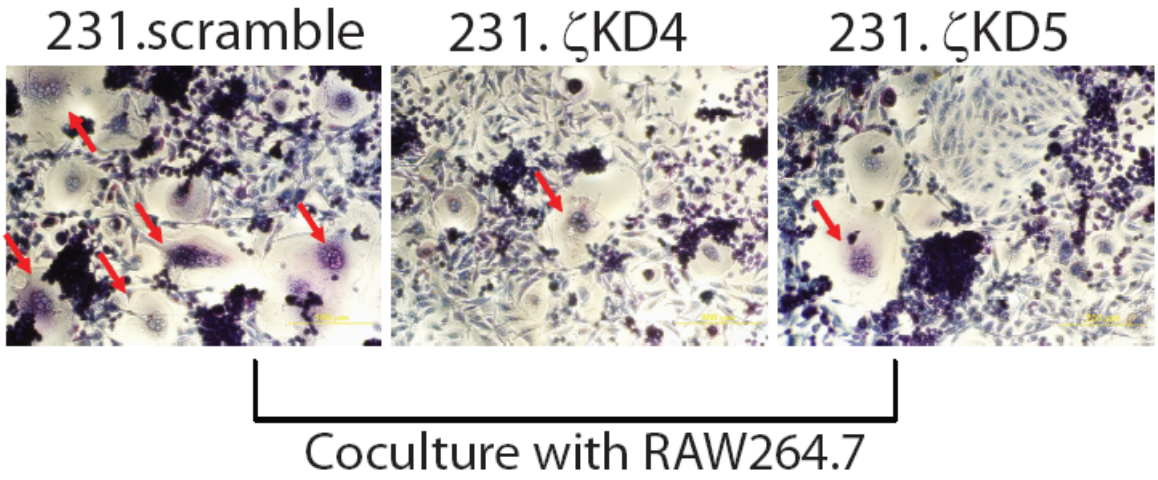

Figure 26. Knockdown of 14-3-3ζ in MDA231 cells inhibits osteoclasts differentiation in the co-culture system with Raw264.7 osteoclast cells.
231.scramble, 231.ζKD4, and 231.ζKD5 cells were co-cultured with RAW264.7 osteoclast cells for 5 days. Representative images of $TRAP^{+}$ staining of osteoclasts from the coculture system. The red arrows indicate mature $TRAP^{+}$ osteoclast cells.

To directly test whether 14-3-3ζ is functionally important for TGF-β-induced breast cancer bone metastasis, I labeled the previously described MDA231 sublines with a GFP-Luciferase reporter and injected these cells into athymic nude mice via intra-tibial injection. The progression of bone metastases was monitored by weekly bioluminescence imaging (BLI). Knockdown of 14-3-3ζ significantly extended survival and delayed the onset of bone metastasis in mice (Fig. 27). I also confirmed the difference in bone tumor burden by BLI measurement, histomorphometric H&E staining, X-ray analysis and IHC staining specific to 14-3-3ζ and 14-3-3σ (Fig. 28). BLI analysis showed that 231 control cells generate bone metastatic colonies by 5 weeks after injection, and almost 90% of injected mice have bone lesions before 7 weeks (Fig. 27). However, only 37.5% of mice injected with 14-3-3ζ knockdown cells generate bone metastatic colonies by the endpoint of the experiment (10 weeks, Fig. 27). Although I found several mice with bone metastasis in the 14-3-3ζ KD group, we found this is due to incomplete knockdown of 14-3-3ζ in those lesions as determined by H&E staining and IHC staining for 14-3-3ζ (data not shown). These could be explained by a possible mechanism that 14-3-3ζ KD cells are heterogeneous, and only those cells with 14-3-3ζ expression and response to TGF-β signaling can be selected out by bone microenvironment from the whole population and thrive. I also collected bone lesions from those mice and stained with Tartrate-resistant acid phosphatase-positive (TRAP+) marker to test whether bone osteolysis is activated in the bone microenviroment. Consistent with our hypothesis, histological analysis demonstrated a significant decrease in the number of TRAP+ osteoclasts along the bone-tumor interface of bone lesions generated by 14-3-3ζ KD cells compared to control cells(data not shown).

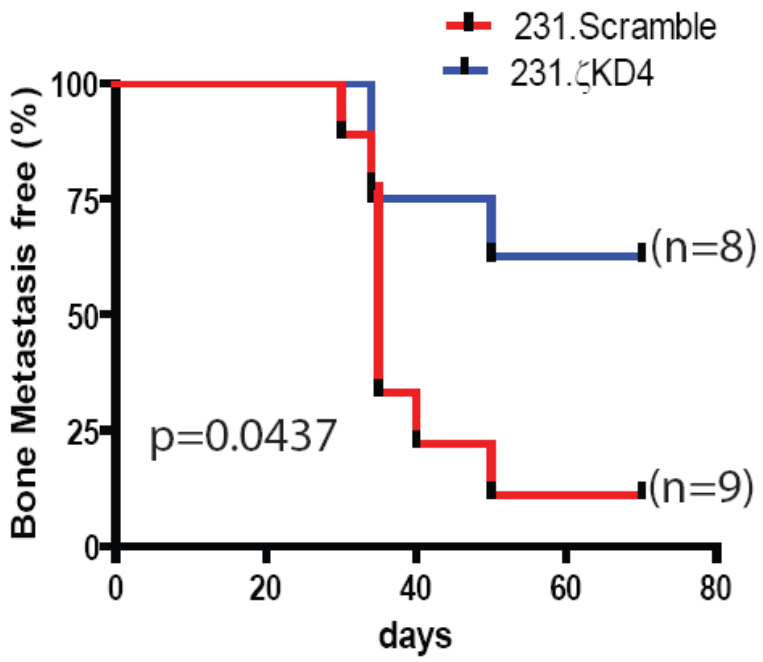

Figure 27. Knockdown of 14-3-3ζ in MDA231 cells inhibits cancer cell metastatic colonization in bone microenvironment.
Kaplan-Meier survival curve of mice (n=10) injected intratibially with 231.scramble or 231.14-3-3ζKD4 cells.

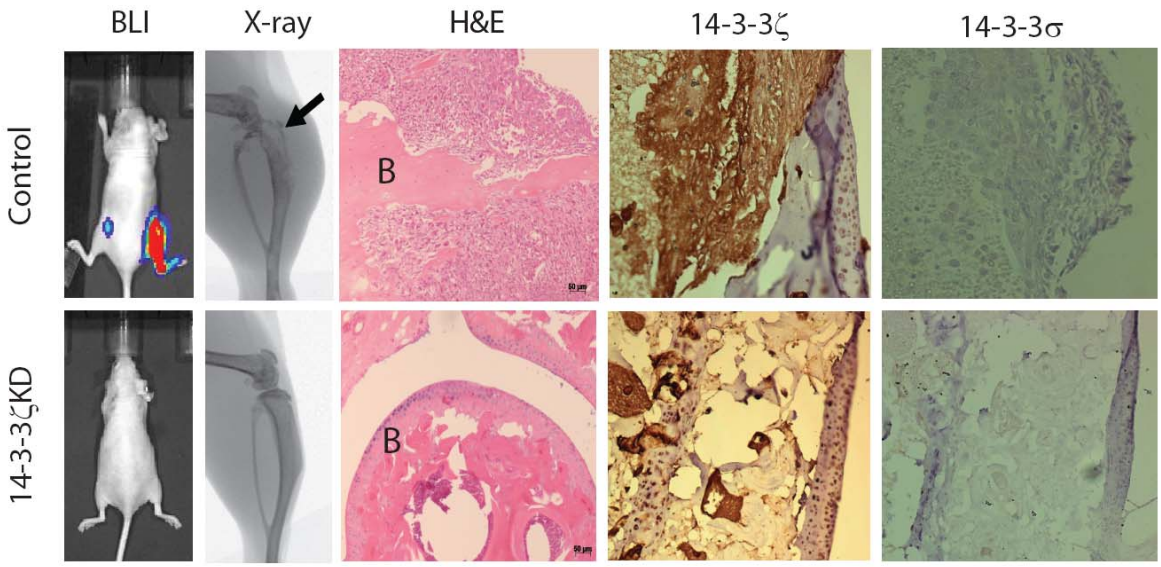

Figure 28. Knockdown of 14-3-3ζ in MDA231 cells inhibits cancer cell metastatic colonization in the bone microenvironment.
BLI, X-ray, and histological (H&E and IHC) images of bone lesions from two representative mice in each experimental group on day 49. Black arrows indicate osteolytic bone lesions in the X-ray images and tumor burden in the histological images. Immunohistochemical representative images for 14-3-3ζ and 14-3-3σ expression are also shown.

TGF-β downstream targets, including PTHrP, IL-11, Jagged-1 and CTGF, have been shown to modulate the invasive and metastatic behavior of MDA231 cells, as well as survival in the bone microenvironment (4, 61-63). Our next step was to identify the downstream targets of the TGF-β signaling pathway which are significantly affected by 14-3-3ζ overexpression. After TGF-β treatment in MDA231 sublines for 2 hours, I found that knockdown of 14-3-3ζ in 231 cells can inhibit TGF-β-induced PTHrP, Jagged-1 and IL-11 transcription. In particular, PTHrP gene expression was dramatically inhibited nearly 3 fold (Fig. 29 & Fig. 30). All of these data suggest that 14-3-3ζ-mediated PTHrP expression in breast cancer cells is critical for TGF-β induced bone metastatic colonization.

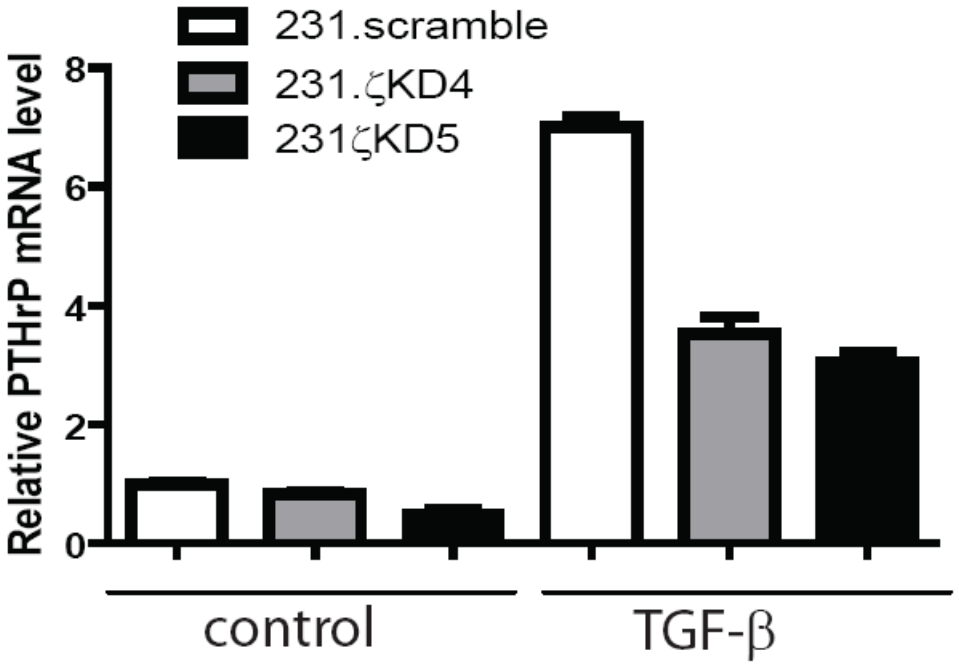

Figure 29. Knockdown of 14-3-3ζ inhibits TGF-β-induced PTHrP gene expression in MDA231 cells.
qRT-PCR analysis of PTHrP mRNA expression in MDA231 cell line and its derivative sublines follwing treatment of TGF-β (5 ng/ml) or vehicle control.

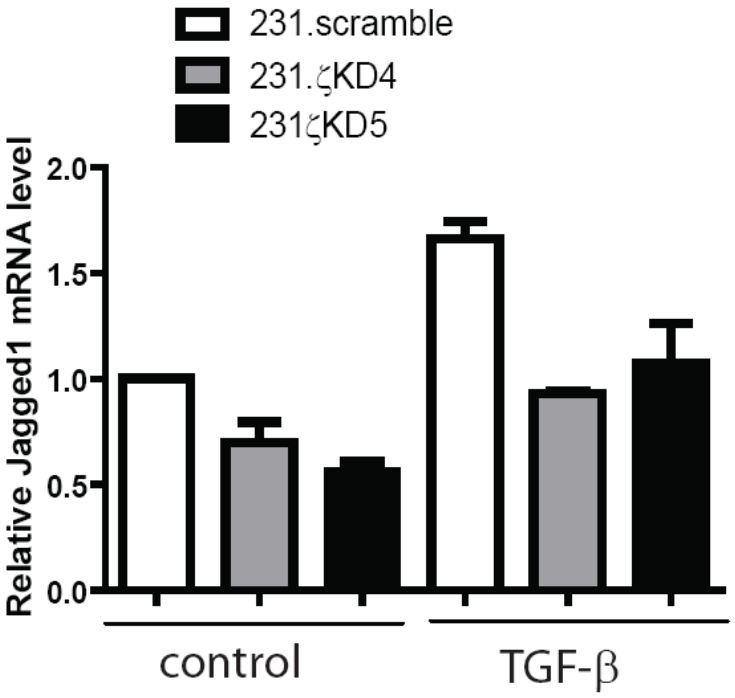

Figure 30. Knockdown of 14-3-3ζ inhibits TGF-β -induced Jagged1 gene expression in MDA231 cells.
qRT-PCR analysis of Jagged1 mRNA expression in MDA231 cells and its derivative sublines following treatment of TGF-β (5 ng/ml) or vehicle control.

Gli2/smad2 complex is required for TGF-β induced PTHrP expression

TGF-β induces PTHrP expression not only through the classical smad2/3/4 signaling pathway, but also through non-canonical signaling cascades such as p38 MAPK (64). There are several reported transcription factors which are responsible for PTHrP gene expression, including Ets1 (65). Overexpression of Gli2 occurs in a variety of cancers and promotes cancer progression via regulation of cell cycle progression and apoptosis(66). A recent study showed that Gli2, which is the most transcriptionally active form of the Gli family, is directly involved in melanoma invasion and metastasis (67). Moreover, TGF-β can induce Gli2 and Gli1 expression through transcriptional activation in breast cancer cell lines (68, 69). Additionally, TGF-β promotes Gli2-induced expression of PTHrP independent of canonical Hedgehog signaling and contributes to breast cancer bone metastasis (70). Runx2 also contributes to TGF-β-mediated tumor growth and osteolysis and colocalizes with Gli2 to further activate PTHrP (71). These data suggest that the TGF-β/smads/Gli2 signaling axis is very important for cancer progression and metastasis (72). However, the mechanism by which Gli2 contributes to TGF-β induced PTHrP expression and the relationship between Gli2 and Smads remains elusive.

To address a potential relationship between these two components in the TGF-β-induced bone metastases program, I treated 231 cells with TGF-β for 2 hours and performed an immunoprecipitation assay using smad2 antibody. Interestingly, I found that Gli2 immediately binds to p-smad2 in response to TGF-β (Fig. 31). However, when 14-3-3ζ was knocked down in MDA231 cells, p-smad2 no longer bound to Gli2 (Fig. 32). Collectively, these data suggest that Gli2 binds to smad2 in response to TGF-β signaling and aids smad

complex recognition and binding to the PTHrP promoter. This Gli2/smad complex is important for TGF-β-induced PTHrP gene expression.

Figure 31. Smad2 binds to Gli2 in MDA231 cells in response to TGF-β treatment. Interaction between Smad2 and Gli2 in MDA231 cells shown by IP-western analysis after treatment with TGF-β (5 ng/ml).

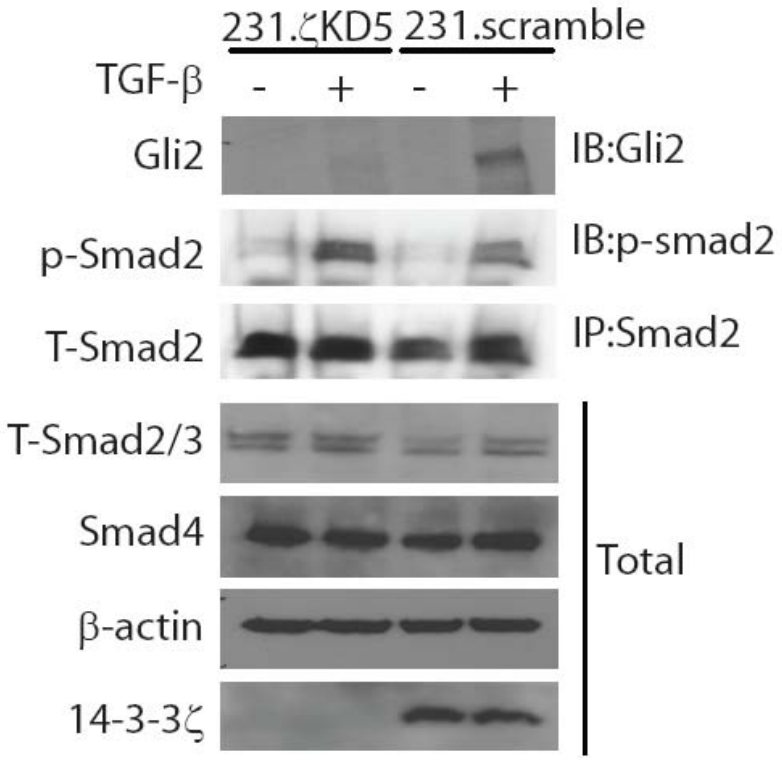

Figure 32. Knockdown of 14-3-3ζ inhibits Smad2 binding to Gli2 in MDA231 cells in response to TGF-β treatment.
Immunoprecipitation of endogenous Gli2 and p-smad2 in 231 and 231.ζKD5 cells upon treatment with TGF-β (5 ng/ml) or vehicle.

Gli2 stabilization by 14-3-3ζ is critical for TGF-β induced PTHrP expression

There are several mechanisms regulating the activity of Gli transcription factors, including nuclear-cytoplasmic shuttling (73, 74), and ubiquitination and protein degradation (75-79). In 231.14-3-3ζKD cells, I found that Gli2 protein level did not increase after TGF-β treatment for 2 hours compared to 231.scramble cells (Fig. 33), while there was no difference in mRNA level between 231.scramble cells and 231.14-3-3ζKD cells (Fig. 34). Additionally, a recent report showed that the mRNA level of Gli2 reaches a peak at 48hr after TGF-β treatment, but protein level increases within 2 hours of TGF-β treatment (69). These findings together with our data suggest that TGF-β may also stabilize Gli2 protein in addition to increasing its gene expression. Thus, we hypothesize that 14-3-3ζ may regulate Gli2 at the protein level in response to TGF-β.

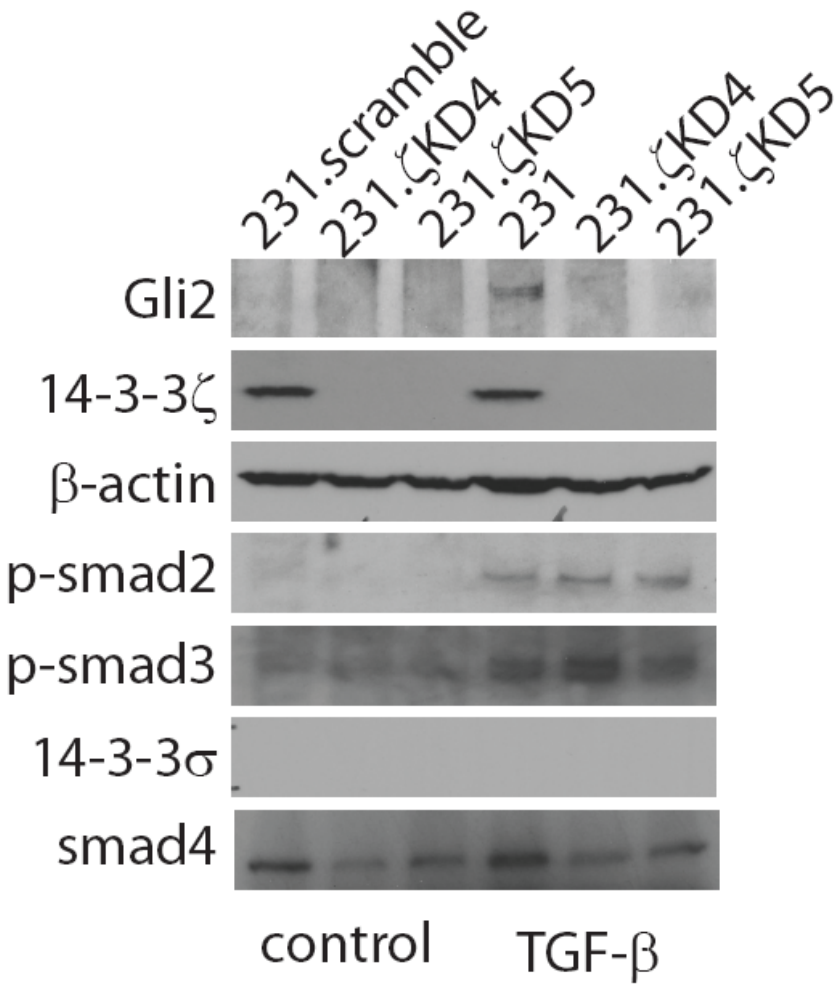

Figure 33. Knockdown of 14-3-3ζ downregulates Gli2 protein level in MDA231 cells in response to TGF-β treatment.
Western blot analysis showing Gli2 and 14-3-3ζ protein levels in the indicated cell lines with treatment of TGF-β (5ng/ml) or vehicle control.

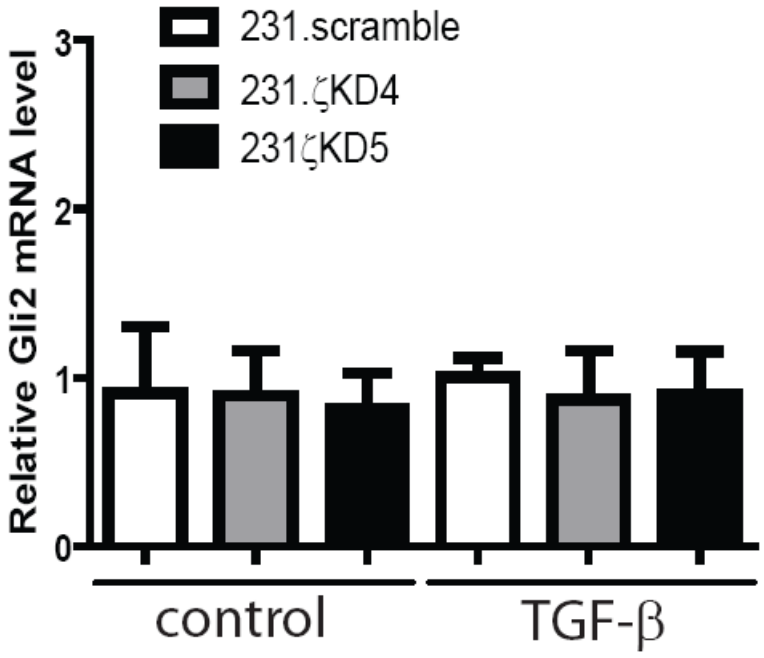

Figure 34. Knockdown of 14-3-3ζ does not change Gli2 mRNA level in MDA231 cells in response to TGF-β treatment.
qRT-PCR analysis of mRNA expression of Gli2 in MDA231 cell line and its derivative sublines upon treatment with TGF-β (5 ng/ml) or vehicle.

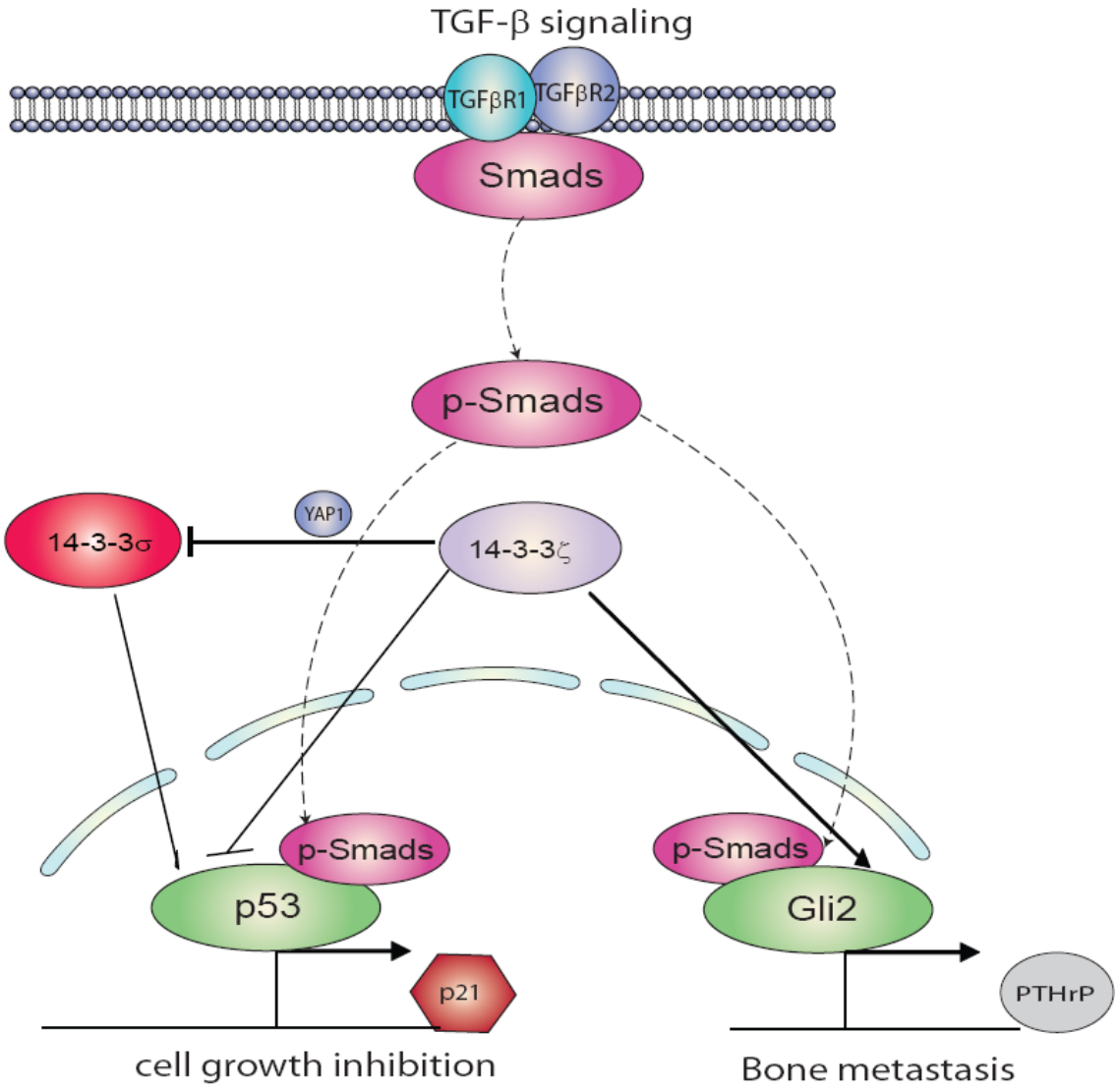

Figure 35. Schematic diagram depicting 14-3-3ζ-mediated switch of TGF-β function.

See text for details.

Chapter 4: Discussion

In this study, I have found that overexpression of 14-3-3ζ inhibits the cytostatic program of TGF-β through destabilizing p53 in non-transformed human mammary epithelial cells. Mechanistically, I found that 14-3-3ζ overexpression leads to 14-3-3σ downregulation, thereby activating the PI3K/Akt signaling pathway, which degrades p53 and further inhibits TGF-β induced p21 expression and cell cytostatic function. In addition, I also found that overexpression of 14-3-3ζ promotes TGF-β-induced breast cancer bone metastatic colonization through stabilizing Gli2, which is an important co-transcriptional factor for p-smad2 to activate PTHrP expression and bone osteolytic effect. Taken together, we reveal a novel mechanism by which 14-3-3ζ dictates the tumor suppressor or metastasis promoter activities of the TGF-β signaling pathway through switching p-smad2's binding partner from p53 to Gli2 (Fig. 35). Our results not only provide a better understanding of the important role of 14-3-3ζ in early stage breast cancer development, but also deeply impact our knowledge of signaling mechanisms underlying the complex roles of TGF-β in cancer, which provides us with a more accurate strategy to determine when and how anti-TGF-β targeted therapy might be effective.

TGF-β's functional switch

In normal epithelial cells, TGF-β induces cytostatic genes, including p15(37) and p21 (38) (39, 40). It also inhibits another category of genes that promote cell growth, including c-myc(41) (42, 43). Our study shows that p21 is the major downstream effector of TGF-β's cytostatic program in MCF-10A cells. However, we cannot exclude other downstream genes that may also contribute to this program. As indicated in our figure 5, p21 knockdown in MCF-10A cells did not make them fully resistant to TGF-β's cytostatic effect. Additionally,

I also found that 14-3-3ζ overexpression inhibits TGF-β induced p15 expression, but MCF-10A cells have only trace levels of p15 protein which could not contribute to TGF-β's cytostatic program dramatically.

It has been well characterized that TGF-β inhibits cell proliferation in normal epithelial cells, but promotes cancer cell metastasis. However, the molecular mechanism by which TGF-β switches its role remained elusive. There were several studies that attempted to address this question, for example, TMEPAI knockdown attenuated TGF-β induced growth and motility in breast cancer cells (80), another report demonstrated that epigenetic downregulation of DAB2 blocked TGF-β-mediated inhibition of cell proliferation and migration in human squamous cells carcinoma (81). However, these studies do not exactly provide evidence to show how TGF-β lost its tumor suppressor function in normal epithelial cells, as the majority of the data were obtained from cancer cell lines such as MDA231 cells, in which TGF-β already executes a tumor promoter function. Additionally, these studies focused primarily on cell proliferation and tumor growth, which is only one of TGF-β's functions, but did not address the metastasis-promoting ability of TGF-β. In our study, we found direct evidence that overexpression of 14-3-3ζ inhibits TGF-β's cell cytostatic program in non-transformed human mammary epithelial cells, while overexpression of 14-3-3ζ promotes TGF-β induced breast cancer bone metastatic colonization. In addition, we reveal a novel mechanism by which 14-3-3ζ dictates the tumor suppressor or metastases promoter activities of the TGF-β signaling pathway through switching p-smad2's binding partner from p53 to Gli2.

Since TGF-β plays an important role in cancer development and a variety of other diseases, a lot of effort has been placed to develop cancer therapeutics to target TGF-β

signaling in both the tumor and its microenvironment. Currently, several kinds of TGF-β signaling antagonists have been developed and applied to clinical practice, the most advanced drug are large molecules, including monoclonal antibodies and antisense oligonucleotides. In addition, there are also several orally bioavailable small molecule kinase inhibitors developed to target this signaling pathway(82). However, as tumors evolve, TGF-β switches its role from being a tumor suppressor to a tumor promoter, and the complex nature and dual roles of TGF-β in cancer has impeded the development of effective therapies that target only the tumor-promoting activities of TGF-β. Understanding the molecular mechanism by which TGF-β switches its role will benefit the development of promising agents and strategies. Previously, we have found that 14-3-3ζ overexpression occurs in the early stage breast cancer development (ADH)(3) and is overexpressed in more that 40% of breast cancer patients which highly correlates with disease recurrence(18). In this study, we found that 14-3-3ζ overexpression in early stage breast cancer development serves as a novel molecular switch that turning TGF-β from tumor suppressor to tumor promoter. This may suggest that the expression level of 14-3-3ζ could serve as a novel molecular biomarker that can aid in the selection of appropriate patients who will benefit from TGF-β antagonists(7), and it may help determining when and how anti-TGF-β targeted therapy might be feasible(6).

p53's convergence with the TGF-β signaling pathway

Although the signal transduction cascade of TGF-β is quite simple compared to other receptor-mediated signal cascades, involving only a few types of smad proteins, the cellular responses to TGF-β are complicated and highly dependent on the cell context. This versatility could be explained by the physical interactions between smads and a remarkable

diversity of DNA sequence-binding transcription factors. To date, those binding partners in mammalian cells include bHLH family, Forkhead family, Zinc finger protein family, and p53 (83). For example, in neuroepithelial and glioblastoma cells, TGF-β induces smad3/4 to form a complex with Foxo3a (38). Sp1 also has been reported to bind with smads to transactivate p15 and p21 gene expression in hepatic cells (39, 40). However, our data combined with other reports (35, 50, 52, 84) show this complex does not exist in human mammary epithelial cells, indicating the TGF-β signaling program is highly cell context-dependent. In our study, we found that p53 collaborates with smad2/3/4 to transactivate p21 gene expression in response to TGF-β in MCF-10A cells. Interestingly, it is reported that TGF-β induces p21 through a p53-independent mechanism in the HaCaT cell line, which contains two mutant alleles of p53 which are unable to activate transcription of p21 (85). Taken together, all of these data suggest that TGF-β's signaling program is highly cell context-dependent.

In our study, we found overexpression of 14-3-3ζ inhibits the cytostatic program of TGF-β through destabilization of p53 in MCF-10A cells. In late stage of breast cancer development, p53 is usually found to be lost or mutated, especially mutant p53 is found in almost 50% of breast cancers (86). 14-3-3ζ overexpression has been found in more than 40% of advanced breast cancers (18) and starts at the early stage of breast cancer development-Atypical Ductal Hyperplasia , which is also the transition phase of TGF-β's function (3, 6). This may suggest that 14-3-3ζ overexpression could be one of the mechanisms leads to downregulation of p53, thereby contributes to inhibition of TGF-β's cytostatic function in the early transition phase of breast cancer development. In addition, p53 mutation also could contribute to TGF-β's function switch. As shown in previous study,

there is a R280K mutation in p53 in MDA231 cells, and this mutant p53 still can form a complex with smads, but empowers TGF-β induced metastasis (35).

14-3-3ζ and 14-3-3σ

In our study, we found a novel mechanism by which 14-3-3ζ overexpression downregulates 14-3-3σ through transcriptional repression. It is interesting that these two proteins belong to the same family, yet the functions of these two members have been well characterized to be opposite. This biological specificity of 14-3-3σ could be explained by the structure difference between 14-3-3σ and the rest of 14-3-3 family members (87, 88). The structure suggests a second ligand binding site (involving residues Met-202, Asp-204, and His-206) involved in 14-3-3σ unique ligand discrimination (87). In addition, most of 14-3-3 family members except 14-3-3σ form homodimers or mixed heterodimers among different isoforms, and they shared the similar ligand binding and function. In contrast, 14-3-3σ only forms homodimers. The structural study also reveals a stabilizing ring-ring and salt bridge interactions involving Lys-9 and Glu-83 unique to the 14-3-3σ, and rationalizes that 14-3-3σ preferentially form homodimer and has destabilized electrostatic interactions with the other members to form heterodimers (87).

Among the 14-3-3 family, 14-3-3 σ is well recognized as a tumor suppressor gene, and is lost in multiple types of cancer (89). Based on our previous findings, 14-3-3ζ overepressed in more than 40% of advanced breast cancer (18)and 14-3-3ζ overexpression defines high risk for breast cancer recurrence and promotes cancer cells survival. Moreover, 14-3-3ζ plays an opposite role with 14-3-3σ in many signaling pathway, including PI3K-Akt pathway, p53 stabilization, glycolysis and metabolism, polarity and invasion. However, the mechanism by which the balance between 14-3-3ζ and 14-3-3σ was broken in mammalian

cell is still unclear. Here, we report that a novel mechanism that 14-3-3ζ overexpression transcriptional repress 14-3-3σ gene expression through sequestering YAP1 transcription factor outside of the nucleus. It would suggest a critical role of YAP1 in maintaining the homeostasis of 14-3-3 family in mammalian cell. When the cells harvest gene amplification of 14-3-3ζ(18), it will disrupt the balance and lead to downregulation of 14-3-3σ, and tissue malfunction and human disease.

The complicate role of YAP1 in Cancer

The Hippo pathway plays an important role in controlling organ size, tissue regeneration, stem cell renew and tumorigenesis (90). The recent findings show that Hippo pathway can be regulated by cell polarity, cell adhesion and cell junction proteins, and activation of Hippo pathway leads to phosphorylation and inhibition of transcription co-activators, such as YAP, TAZ, and Yki(91). In mammalian cell, YAP phosphorylated by Lats1/2 at Ser127 site and binds to 14-3-3 leads to subsequent cytoplasmic sequestration and inactivation (91). However, there is an argument of YAP's role in cancer development. Initially, YAP was defined as a tumor suppressor supported by the evidence of working together with p73, PML to induce apoptosis in response to DNA damage (92-95). The new concept of YAP1 as an oncogene emerge recently as supported by amplification in human HCC(96) and transformation ability of YAP in MCF-10A cells(97). The different role of YAP in cancer development might be cell context-specific and binding partners dependent. As a transcriptional co-activator, YAP1 functions when it is bound to different transcription factors. YAP functions as oncogene when it binds to TEAD family transcription factors in regulation of CTGF gene expression which promotes cell proliferation (98). In contrast, it functions as a tumor suppressor when YAP binding to p73 or p53BP2, which is then

inhibited by Akt phosphorylation (56). In our study, I found that 14-3-3ζ overexpression downregulates 14-3-3σ through sequestering YAP1 in the cytosol, which suggests that YAP1 transactivates 14-3-3σ when located in the nucleus. However, the transcription factor which YAP binds to and collaborates with to activate 14-3-3σ gene expression is still unknown. In our study, I found that YAP protein level was not altered by 14-3-3ζ overexpression, but subcellular localization was changed. On the other hand, majority of data suggest YAP1 serves as an oncogene in nucleus, but this does not exclude the possibility that YAP1 also function as an oncogene in the cytosol, which is primarily retained by 14-3-3 binding. In the study that shown the transformation ability of YAP in MCF-10A cells, the exactly localization of YAP that executes the oncogene function is not clearly stated (97).

Chapter 5: Future studies

In our study, we found that p53 binds to smad2/3/4 together in response to TGF-β in MCF-10A cells. However, it has been reported that TGF-β induces p21 through a p53-independent mechanism in HaCaT cell line which contains two mutant alleles of p53, which are unable to activate transcription of p21(85). These data would suggest that the cellular responses to TGF-β are complicate and highly cell context dependent. To determine if p53 is critical for TGF-β induced p21 gene expression in human mammary epithelial cells, I will knockdown p53 in MCF-10A cells to see if it impairs TGF-β induced p21 gene expression. In addition, it is also necessary to determine if mutant p53 binds to smads in MDA231 cells and identify the downstream signaling cascade in late stage of breast cancer development. These data will further indicate the critical role of p53 in TGF-β's cytostatic program and support our hypothesis that 14-3-3ζ overexpression switches off TGF-β's cytostatic program through 14-3-3σ downregulation and destabilization of p53.

TGF-β can induce Gli2 and Gli1 expression through transcriptional activation in breast cancer cell lines (68, 69), and it promotes Gli2-induced expression of PTHrP and contributes to breast cancer bone metastasis (70). These data suggest that the TGF-β/smads/GLi2 signaling axis is very import for cancer progression and metastasis (72). However, the mechanism by which Gli2 contributes to TGF-β induced PTHrP expression and the convergence effect between Gli2 and Smads remains elusive. It is the first time shown that Gli2 binds to smad2 in response to TGF-β in breast cancer cells as indicated in our data. To further determine the important role of Gli2 as a co-transcription factor to smads and contribution to TGF-β's metastatic program, it is necessary to knockdown Gli2 in MDA231 cells to test if it can impair TGF-β induced PTHrP gene expression. In addition, to determine

if this smad2/Gli2 complex is critical for PTHrP gene transcription in response to TGF-β and whether the complex could be disrupted by 14-3-3ζ knockdown in MDA231 cells, I will perform a ChIP assay on the promoter region of PTHrP using specific antibodies recognizing Gli2 or smad2 under TGF-β stimulation.

In 231.14-3-3ζKD cells, I found that Gli2 protein level was dramatically decreased compared to 231.scramble cells after TGF-β treatment for 2 hours but there are no difference on mRNA level between 231.scramble cells and 231.14-3-3ζKD cells. These data suggest that 14-3-3ζ may regulate Gli2 protein stability in response to TGF-β. As previous study shown that Gli2 is targeted for ubiquitination and degradation by β-TrCP Ubiquitin Ligase(99). First, I will test if Gli2 has increased ubiquitination in MDA231.14-3-3ζKD cells compared to MDA231 control cells. Next, I will investigate the mechanism by which 14-3-3ζ overexpression prevents Gli2 to be targeted for ubiquitination and degradation by β-TrCP Ubiquitin Ligase.

14-3-3ζ has been knockdown in MDA231 cells to test if lost of 14-3-3ζ can impair TGF-β induced breast cancer cells bone metastasis. To further confirm that 14-3-3ζ overexpression promotes TGF-β induced breast cancer cells bone metastasis, I will also overexpress 14-3-3ζ in McNeuA cells which is derived from MMTV-Neu mice and has equal amount of 14-3-3ζ expression as MCF-10A cells, and challenge these GFP-Luciferase labeled McNeuA control cells and McNeuA.14-3-3ζ cells to in vivo bone metastatic colonization through intra-tibial injection test if 14-3-3ζ overexpression can promote TGF-β mediated McNeuA cells bone metastasis. In addition, I will also treat the mice injected with McNeuA.14-3-3ζ cells with TGF-βR inhibitor (LY2109761, Eli Lilly) to test if the increased bone metastasis is due to upregulated TGF-β signaling mediated by 14-3-3ζ overexpression.

This data would be expected to strengthen our hypothesis that 14-3-3ζ overexpression switches on TGF-β induced breast cancer cells bone metastasis program.

Bibliography:

1. Burstein, H. J., K. Polyak, J. S. Wong, S. C. Lester, and C. M. Kaelin. 2004. Ductal carcinoma in situ of the breast. N Engl J Med 350:1430-1441.
2. Polyak, K. 2001. On the birth of breast cancer. Biochim Biophys Acta 1552:1-13.
3. Danes, C. G., S. L. Wyszomierski, J. Lu, C. L. Neal, W. Yang, and D. Yu. 2008. 14-3-3 zeta down-regulates p53 in mammary epithelial cells and confers luminal filling. Cancer Res 68:1760-1767.
4. Yin, J. J., K. Selander, J. M. Chirgwin, M. Dallas, B. G. Grubbs, R. Wieser, J. Massague, G. R. Mundy, and T. A. Guise. 1999. TGF-beta signaling blockade inhibits PTHrP secretion by breast cancer cells and bone metastases development. J Clin Invest 103:197-206.
5. Siegel, P. M., and J. Massague. 2003. Cytostatic and apoptotic actions of TGF-beta in homeostasis and cancer. Nat Rev Cancer 3:807-821.
6. Massague, J. 2008. TGFbeta in Cancer. Cell 134:215-230.
7. Arteaga, C. L. 2006. Inhibition of TGFbeta signaling in cancer therapy. Curr Opin Genet Dev 16:30-37.
8. Bierie, B., and H. L. Moses. 2006. Tumour microenvironment: TGFbeta: the molecular Jekyll and Hyde of cancer. Nat Rev Cancer 6:506-520.
9. Wrzesinski, S. H., Y. Y. Wan, and R. A. Flavell. 2007. Transforming growth factor-beta and the immune response: implications for anticancer therapy. Clin Cancer Res 13:5262-5270.
10. Aitken, A. 2006. 14-3-3 proteins: a historic overview. Semin Cancer Biol 16:162-172.

11. Tzivion, G., Z. Luo, and J. Avruch. 1998. A dimeric 14-3-3 protein is an essential cofactor for Raf kinase activity. Nature 394:88-92.

12. Yaffe, M. B. 2002. How do 14-3-3 proteins work?-- Gatekeeper phosphorylation and the molecular anvil hypothesis. FEBS Lett 513:53-57.

13. Jones, D. H., S. Ley, and A. Aitken. 1995. Isoforms of 14-3-3 protein can form homo- and heterodimers in vivo and in vitro: implications for function as adapter proteins. FEBS Lett 368:55-58.

14. Porter, G. W., F. R. Khuri, and H. Fu. 2006. Dynamic 14-3-3/client protein interactions integrate survival and apoptotic pathways. Semin Cancer Biol 16:193-202.

15. Liu, D., J. Bienkowska, C. Petosa, R. J. Collier, H. Fu, and R. Liddington. 1995. Crystal structure of the zeta isoform of the 14-3-3 protein. Nature 376:191-194.

16. Hermeking, H., C. Lengauer, K. Polyak, T. C. He, L. Zhang, S. Thiagalingam, K. W. Kinzler, and B. Vogelstein. 1997. 14-3-3 sigma is a p53-regulated inhibitor of G2/M progression. Mol Cell 1:3-11.

17. Neal, C. L., J. Xu, P. Li, S. Mori, J. Yang, N. N. Neal, X. Zhou, S. L. Wyszomierski, and D. Yu. Overexpression of 14-3-3zeta in cancer cells activates PI3K via binding the p85 regulatory subunit. Oncogene 31:897-906.

18. Neal, C. L., J. Yao, W. Yang, X. Zhou, N. T. Nguyen, J. Lu, C. G. Danes, H. Guo, K. H. Lan, J. Ensor, W. Hittelman, M. C. Hung, and D. Yu. 2009. 14-3-3zeta overexpression defines high risk for breast cancer recurrence and promotes cancer cell survival. Cancer Res 69:3425-3432.

19. Lu, J., H. Guo, W. Treekitkarnmongkol, P. Li, J. Zhang, B. Shi, C. Ling, X. Zhou, T. Chen, P. J. Chiao, X. Feng, V. L. Seewaldt, W. J. Muller, A. Sahin, M. C. Hung, and D. Yu. 2009. 14-3-3zeta Cooperates with ErbB2 to promote ductal carcinoma in situ progression to invasive breast cancer by inducing epithelial-mesenchymal transition. Cancer Cell 16:195-207.

20. Taylor, W. R., and G. R. Stark. 2001. Regulation of the G2/M transition by p53. Oncogene 20:1803-1815.

21. Yang, A., M. Kaghad, Y. Wang, E. Gillett, M. D. Fleming, V. Dotsch, N. C. Andrews, D. Caput, and F. McKeon. 1998. p63, a p53 homolog at 3q27-29, encodes multiple products with transactivating, death-inducing, and dominant-negative activities. Mol Cell 2:305-316.

22. Pellegrini, G., E. Dellambra, O. Golisano, E. Martinelli, I. Fantozzi, S. Bondanza, D. Ponzin, F. McKeon, and M. De Luca. 2001. p63 identifies keratinocyte stem cells. Proc Natl Acad Sci U S A 98:3156-3161.

23. Westfall, M. D., D. J. Mays, J. C. Sniezek, and J. A. Pietenpol. 2003. The Delta Np63 alpha phosphoprotein binds the p21 and 14-3-3 sigma promoters in vivo and has transcriptional repressor activity that is reduced by Hay-Wells syndrome-derived mutations. Mol Cell Biol 23:2264-2276.

24. Urano, T., T. Saito, T. Tsukui, M. Fujita, T. Hosoi, M. Muramatsu, Y. Ouchi, and S. Inoue. 2002. Efp targets 14-3-3 sigma for proteolysis and promotes breast tumour growth. Nature 417:871-875.

25. Ferguson, A. T., E. Evron, C. B. Umbricht, T. K. Pandita, T. A. Chan, H. Hermeking, J. R. Marks, A. R. Lambers, P. A. Futreal, M. R. Stampfer, and S.

Sukumar. 2000. High frequency of hypermethylation at the 14-3-3 sigma locus leads to gene silencing in breast cancer. Proc Natl Acad Sci U S A 97:6049-6054.

26. Suzuki, H., F. Itoh, M. Toyota, T. Kikuchi, H. Kakiuchi, and K. Imai. 2000. Inactivation of the 14-3-3 sigma gene is associated with 5' CpG island hypermethylation in human cancers. Cancer Res 60:4353-4357.

27. Iwata, N., H. Yamamoto, S. Sasaki, F. Itoh, H. Suzuki, T. Kikuchi, H. Kaneto, S. Iku, I. Ozeki, Y. Karino, T. Satoh, J. Toyota, M. Satoh, T. Endo, and K. Imai. 2000. Frequent hypermethylation of CpG islands and loss of expression of the 14-3-3 sigma gene in human hepatocellular carcinoma. Oncogene 19:5298-5302.

28. Umbricht, C. B., E. Evron, E. Gabrielson, A. Ferguson, J. Marks, and S. Sukumar. 2001. Hypermethylation of 14-3-3 sigma (stratifin) is an early event in breast cancer. Oncogene 20:3348-3353.

29. Gasco, M., A. Sullivan, C. Repellin, L. Brooks, P. J. Farrell, J. A. Tidy, B. Dunne, B. Gusterson, D. J. Evans, and T. Crook. 2002. Coincident inactivation of 14-3-3sigma and p16INK4a is an early event in vulval squamous neoplasia. Oncogene 21:1876-1881.

30. Gasco, M., A. K. Bell, V. Heath, A. Sullivan, P. Smith, L. Hiller, I. Yulug, G. Numico, M. Merlano, P. J. Farrell, M. Tavassoli, B. Gusterson, and T. Crook. 2002. Epigenetic inactivation of 14-3-3 sigma in oral carcinoma: association with p16(INK4a) silencing and human papillomavirus negativity. Cancer Res 62:2072-2076.

31. Feng, W., L. Shen, S. Wen, D. G. Rosen, J. Jelinek, X. Hu, S. Huan, M. Huang, J. Liu, A. A. Sahin, K. K. Hunt, R. C. Bast, Jr., Y. Shen, J. P. Issa, and Y. Yu. 2007.

Correlation between CpG methylation profiles and hormone receptor status in breast cancers. Breast Cancer Res 9:R57.

32. Lodygin, D., and H. Hermeking. 2005. The role of epigenetic inactivation of 14-3-3sigma in human cancer. Cell Res 15:237-246.

33. Lodygin, D., A. S. Yazdi, C. A. Sander, T. Herzinger, and H. Hermeking. 2003. Analysis of 14-3-3sigma expression in hyperproliferative skin diseases reveals selective loss associated with CpG-methylation in basal cell carcinoma. Oncogene 22:5519-5524.

34. Zhu, F., X. Xia, B. Liu, J. Shen, Y. Hu, and M. Person. 2007. IKKalpha shields 14-3-3sigma, a G(2)/M cell cycle checkpoint gene, from hypermethylation, preventing its silencing. Mol Cell 27:214-227.

35. Adorno, M., M. Cordenonsi, M. Montagner, S. Dupont, C. Wong, B. Hann, A. Solari, S. Bobisse, M. B. Rondina, V. Guzzardo, A. R. Parenti, A. Rosato, S. Bicciato, A. Balmain, and S. Piccolo. 2009. A Mutant-p53/Smad complex opposes p63 to empower TGFbeta-induced metastasis. Cell 137:87-98.

36. Ikushima, H., and K. Miyazono. TGFbeta signalling: a complex web in cancer progression. Nat Rev Cancer 10:415-424.

37. Seoane, J., C. Pouponnot, P. Staller, M. Schader, M. Eilers, and J. Massague. 2001. TGFbeta influences Myc, Miz-1 and Smad to control the CDK inhibitor p15INK4b. Nat Cell Biol 3:400-408.

38. Seoane, J., H. V. Le, L. Shen, S. A. Anderson, and J. Massague. 2004. Integration of Smad and forkhead pathways in the control of neuroepithelial and glioblastoma cell proliferation. Cell 117:211-223.

39. Pardali, K., A. Kurisaki, A. Moren, P. ten Dijke, D. Kardassis, and A. Moustakas. 2000. Role of Smad proteins and transcription factor Sp1 in p21(Waf1/Cip1) regulation by transforming growth factor-beta. J Biol Chem 275:29244-29256.

40. Moustakas, A., and D. Kardassis. 1998. Regulation of the human p21/WAF1/Cip1 promoter in hepatic cells by functional interactions between Sp1 and Smad family members. Proc Natl Acad Sci U S A 95:6733-6738.

41. Chen, C. R., Y. Kang, P. M. Siegel, and J. Massague. 2002. E2F4/5 and p107 as Smad cofactors linking the TGFbeta receptor to c-myc repression. Cell 110:19-32.

42. Claassen, G. F., and S. R. Hann. 2000. A role for transcriptional repression of p21CIP1 by c-Myc in overcoming transforming growth factor beta -induced cell-cycle arrest. Proc Natl Acad Sci U S A 97:9498-9503.

43. Chen, C. R., Y. Kang, and J. Massague. 2001. Defective repression of c-myc in breast cancer cells: A loss at the core of the transforming growth factor beta growth arrest program. Proc Natl Acad Sci U S A 98:992-999.

44. Kang, Y., C. R. Chen, and J. Massague. 2003. A self-enabling TGFbeta response coupled to stress signaling: Smad engages stress response factor ATF3 for Id1 repression in epithelial cells. Mol Cell 11:915-926.

45. Vincent, T., E. P. Neve, J. R. Johnson, A. Kukalev, F. Rojo, J. Albanell, K. Pietras, I. Virtanen, L. Philipson, P. L. Leopold, R. G. Crystal, A. G. de Herreros, A. Moustakas, R. F. Pettersson, and J. Fuxe. 2009. A SNAIL1-SMAD3/4 transcriptional repressor complex promotes TGF-beta mediated epithelial-mesenchymal transition. Nat Cell Biol 11:943-950.

46. Thuault, S., U. Valcourt, M. Petersen, G. Manfioletti, C. H. Heldin, and A. Moustakas. 2006. Transforming growth factor-beta employs HMGA2 to elicit epithelial-mesenchymal transition. J Cell Biol 174:175-183.

47. Shirakihara, T., M. Saitoh, and K. Miyazono. 2007. Differential regulation of epithelial and mesenchymal markers by deltaEF1 proteins in epithelial mesenchymal transition induced by TGF-beta. Mol Biol Cell 18:3533-3544.

48. Comijn, J., G. Berx, P. Vermassen, K. Verschueren, L. van Grunsven, E. Bruyneel, M. Mareel, D. Huylebroeck, and F. van Roy. 2001. The two-handed E box binding zinc finger protein SIP1 downregulates E-cadherin and induces invasion. Mol Cell 7:1267-1278.

49. Brunet, A., A. Bonni, M. J. Zigmond, M. Z. Lin, P. Juo, L. S. Hu, M. J. Anderson, K. C. Arden, J. Blenis, and M. E. Greenberg. 1999. Akt promotes cell survival by phosphorylating and inhibiting a Forkhead transcription factor. Cell 96:857-868.

50. Cordenonsi, M., M. Montagner, M. Adorno, L. Zacchigna, G. Martello, A. Mamidi, S. Soligo, S. Dupont, and S. Piccolo. 2007. Integration of TGF-beta and Ras/MAPK signaling through p53 phosphorylation. Science 315:840-843.

51. Dupont, S., L. Zacchigna, M. Adorno, S. Soligo, D. Volpin, S. Piccolo, and M. Cordenonsi. 2004. Convergence of p53 and TGF-beta signaling networks. Cancer Lett 213:129-138.

52. Cordenonsi, M., S. Dupont, S. Maretto, A. Insinga, C. Imbriano, and S. Piccolo. 2003. Links between tumor suppressors: p53 is required for TGF-beta gene responses by cooperating with Smads. Cell 113:301-314.

53. Yang, H., Y. Y. Wen, R. Zhao, Y. L. Lin, K. Fournier, H. Y. Yang, Y. Qiu, J. Diaz, C. Laronga, and M. H. Lee. 2006. DNA damage-induced protein 14-3-3 sigma inhibits protein kinase B/Akt activation and suppresses Akt-activated cancer. Cancer Res 66:3096-3105.

54. Yang, H. Y., Y. Y. Wen, C. H. Chen, G. Lozano, and M. H. Lee. 2003. 14-3-3 sigma positively regulates p53 and suppresses tumor growth. Mol Cell Biol 23:7096-7107.

55. Hermeking, H., and A. Benzinger. 2006. 14-3-3 proteins in cell cycle regulation. Semin Cancer Biol 16:183-192.

56. Basu, S., N. F. Totty, M. S. Irwin, M. Sudol, and J. Downward. 2003. Akt phosphorylates the Yes-associated protein, YAP, to induce interaction with 14-3-3 and attenuation of p73-mediated apoptosis. Mol Cell 11:11-23.

57. Roodman, G. D. 2004. Mechanisms of bone metastasis. N Engl J Med 350:1655-1664.

58. Kang, Y. 2006. Pro-metastasis function of TGFbeta mediated by the Smad pathway. J Cell Biochem 98:1380-1390.

59. Mourskaia, A. A., Z. Dong, S. Ng, M. Banville, J. C. Zwaagstra, M. D. O'Connor-McCourt, and P. M. Siegel. 2009. Transforming growth factor-beta1 is the predominant isoform required for breast cancer cell outgrowth in bone. Oncogene 28:1005-1015.

60. Padua, D., and J. Massague. 2009. Roles of TGFbeta in metastasis. Cell Res 19:89-102.

61. Sethi, N., X. Dai, C. G. Winter, and Y. Kang. Tumor-derived JAGGED1 promotes osteolytic bone metastasis of breast cancer by engaging notch signaling in bone cells. Cancer Cell 19:192-205.

62. Kang, Y., W. He, S. Tulley, G. P. Gupta, I. Serganova, C. R. Chen, K. Manova-Todorova, R. Blasberg, W. L. Gerald, and J. Massague. 2005. Breast cancer bone metastasis mediated by the Smad tumor suppressor pathway. Proc Natl Acad Sci U S A 102:13909-13914.

63. Kang, Y., P. M. Siegel, W. Shu, M. Drobnjak, S. M. Kakonen, C. Cordon-Cardo, T. A. Guise, and J. Massague. 2003. A multigenic program mediating breast cancer metastasis to bone. Cancer Cell 3:537-549.

64. Kakonen, S. M., K. S. Selander, J. M. Chirgwin, J. J. Yin, S. Burns, W. A. Rankin, B. G. Grubbs, M. Dallas, Y. Cui, and T. A. Guise. 2002. Transforming growth factor-beta stimulates parathyroid hormone-related protein and osteolytic metastases via Smad and mitogen-activated protein kinase signaling pathways. J Biol Chem 277:24571-24578.

65. Lindemann, R. K., P. Ballschmieter, A. Nordheim, and J. Dittmer. 2001. Transforming growth factor beta regulates parathyroid hormone-related protein expression in MDA-MB-231 breast cancer cells through a novel Smad/Ets synergism. J Biol Chem 276:46661-46670.

66. Yang, L., G. Xie, Q. Fan, and J. Xie. Activation of the hedgehog-signaling pathway in human cancer and the clinical implications. Oncogene 29:469-481.

67. Alexaki, V. I., D. Javelaud, L. C. Van Kempen, K. S. Mohammad, S. Dennler, F. Luciani, K. S. Hoek, P. Juarez, J. S. Goydos, P. J. Fournier, C. Sibon, C. Bertolotto,

F. Verrecchia, S. Saule, V. Delmas, R. Ballotti, L. Larue, P. Saiag, T. A. Guise, and A. Mauviel. GLI2-mediated melanoma invasion and metastasis. J Natl Cancer Inst 102:1148-1159.

68. Dennler, S., J. Andre, F. Verrecchia, and A. Mauviel. 2009. Cloning of the human GLI2 Promoter: transcriptional activation by transforming growth factor-beta via SMAD3/beta-catenin cooperation. J Biol Chem 284:31523-31531.

69. Dennler, S., J. Andre, I. Alexaki, A. Li, T. Magnaldo, P. ten Dijke, X. J. Wang, F. Verrecchia, and A. Mauviel. 2007. Induction of sonic hedgehog mediators by transforming growth factor-beta: Smad3-dependent activation of Gli2 and Gli1 expression in vitro and in vivo. Cancer Res 67:6981-6986.

70. Johnson, R. W., M. P. Nguyen, S. S. Padalecki, B. G. Grubbs, A. R. Merkel, B. O. Oyajobi, L. M. Matrisian, G. R. Mundy, and J. A. Sterling. TGF-beta promotion of Gli2-induced expression of parathyroid hormone-related protein, an important osteolytic factor in bone metastasis, is independent of canonical Hedgehog signaling. Cancer Res 71:822-831.

71. Pratap, J., J. J. Wixted, T. Gaur, S. K. Zaidi, J. Dobson, K. D. Gokul, S. Hussain, A. J. van Wijnen, J. L. Stein, G. S. Stein, and J. B. Lian. 2008. Runx2 transcriptional activation of Indian Hedgehog and a downstream bone metastatic pathway in breast cancer cells. Cancer Res 68:7795-7802.

72. Javelaud, D., V. I. Alexaki, S. Dennler, K. S. Mohammad, T. A. Guise, and A. Mauviel. TGF-beta/SMAD/GLI2 signaling axis in cancer progression and metastasis. Cancer Res 71:5606-5610.

73. Sheng, T., S. Chi, X. Zhang, and J. Xie. 2006. Regulation of Gli1 localization by the cAMP/protein kinase A signaling axis through a site near the nuclear localization signal. J Biol Chem 281:9-12.

74. Kogerman, P., T. Grimm, L. Kogerman, D. Krause, A. B. Unden, B. Sandstedt, R. Toftgard, and P. G. Zaphiropoulos. 1999. Mammalian suppressor-of-fused modulates nuclear-cytoplasmic shuttling of Gli-1. Nat Cell Biol 1:312-319.

75. Di Marcotullio, L., E. Ferretti, A. Greco, E. De Smaele, A. Po, M. A. Sico, M. Alimandi, G. Giannini, M. Maroder, I. Screpanti, and A. Gulino. 2006. Numb is a suppressor of Hedgehog signalling and targets Gli1 for Itch-dependent ubiquitination. Nat Cell Biol 8:1415-1423.

76. Huntzicker, E. G., I. S. Estay, H. Zhen, L. A. Lokteva, P. K. Jackson, and A. E. Oro. 2006. Dual degradation signals control Gli protein stability and tumor formation. Genes Dev 20:276-281.

77. Jiang, J. 2006. Regulation of Hh/Gli signaling by dual ubiquitin pathways. Cell Cycle 5:2457-2463.

78. Pan, Y., C. B. Bai, A. L. Joyner, and B. Wang. 2006. Sonic hedgehog signaling regulates Gli2 transcriptional activity by suppressing its processing and degradation. Mol Cell Biol 26:3365-3377.

79. Wang, B., and Y. Li. 2006. Evidence for the direct involvement of {beta}TrCP in Gli3 protein processing. Proc Natl Acad Sci U S A 103:33-38.

80. Singha, P. K., I. T. Yeh, M. A. Venkatachalam, and P. Saikumar. Transforming growth factor-beta (TGF-beta)-inducible gene TMEPAI converts TGF-beta from a tumor suppressor to a tumor promoter in breast cancer. Cancer Res 70:6377-6383.

81. Hannigan, A., P. Smith, G. Kalna, C. Lo Nigro, C. Orange, D. I. O'Brien, R. Shah, N. Syed, L. C. Spender, B. Herrera, J. K. Thurlow, L. Lattanzio, M. Monteverde, M. E. Maurer, F. M. Buffa, J. Mann, D. C. Chu, C. M. West, M. Patridge, K. A. Oien, J. A. Cooper, M. C. Frame, A. L. Harris, L. Hiller, L. J. Nicholson, M. Gasco, T. Crook, and G. J. Inman. Epigenetic downregulation of human disabled homolog 2 switches TGF-beta from a tumor suppressor to a tumor promoter. J Clin Invest 120:2842-2857.

82. Yingling, J. M., K. L. Blanchard, and J. S. Sawyer. 2004. Development of TGF-beta signalling inhibitors for cancer therapy. Nat Rev Drug Discov 3:1011-1022.

83. Feng, X. H., and R. Derynck. 2005. Specificity and versatility in tgf-beta signaling through Smads. Annu Rev Cell Dev Biol 21:659-693.

84. Piccolo, S. 2008. p53 regulation orchestrates the TGF-beta response. Cell 133:767-769.

85. Datto, M. B., Y. Li, J. F. Panus, D. J. Howe, Y. Xiong, and X. F. Wang. 1995. Transforming growth factor beta induces the cyclin-dependent kinase inhibitor p21 through a p53-independent mechanism. Proc Natl Acad Sci U S A 92:5545-5549.

86. Hollstein, M., D. Sidransky, B. Vogelstein, and C. C. Harris. 1991. p53 mutations in human cancers. Science 253:49-53.

87. Wilker, E. W., R. A. Grant, S. C. Artim, and M. B. Yaffe. 2005. A structural basis for 14-3-3sigma functional specificity. J Biol Chem 280:18891-18898.

88. Benzinger, A., G. M. Popowicz, J. K. Joy, S. Majumdar, T. A. Holak, and H. Hermeking. 2005. The crystal structure of the non-liganded 14-3-3sigma protein:

insights into determinants of isoform specific ligand binding and dimerization. Cell Res 15:219-227.

89. Akahira, J., Y. Sugihashi, T. Suzuki, K. Ito, H. Niikura, T. Moriya, M. Nitta, H. Okamura, S. Inoue, H. Sasano, K. Okamura, and N. Yaegashi. 2004. Decreased expression of 14-3-3 sigma is associated with advanced disease in human epithelial ovarian cancer: its correlation with aberrant DNA methylation. Clin Cancer Res 10:2687-2693.

90. Zhao, B., K. Tumaneng, and K. L. Guan. The Hippo pathway in organ size control, tissue regeneration and stem cell self-renewal. Nat Cell Biol 13:877-883.

91. Zhao, B., X. Wei, W. Li, R. S. Udan, Q. Yang, J. Kim, J. Xie, T. Ikenoue, J. Yu, L. Li, P. Zheng, K. Ye, A. Chinnaiyan, G. Halder, Z. C. Lai, and K. L. Guan. 2007. Inactivation of YAP oncoprotein by the Hippo pathway is involved in cell contact inhibition and tissue growth control. Genes Dev 21:2747-2761.

92. Lapi, E., S. Di Agostino, S. Donzelli, H. Gal, E. Domany, G. Rechavi, P. P. Pandolfi, D. Givol, S. Strano, X. Lu, and G. Blandino. 2008. PML, YAP, and p73 are components of a proapoptotic autoregulatory feedback loop. Mol Cell 32:803-814.

93. Strano, S., O. Monti, N. Pediconi, A. Baccarini, G. Fontemaggi, E. Lapi, F. Mantovani, A. Damalas, G. Citro, A. Sacchi, G. Del Sal, M. Levrero, and G. Blandino. 2005. The transcriptional coactivator Yes-associated protein drives p73 gene-target specificity in response to DNA Damage. Mol Cell 18:447-459.

94. Yuan, M., V. Tomlinson, R. Lara, D. Holliday, C. Chelala, T. Harada, R. Gangeswaran, C. Manson-Bishop, P. Smith, S. A. Danovi, O. Pardo, T. Crook, C. A.

Mein, N. R. Lemoine, L. J. Jones, and S. Basu. 2008. Yes-associated protein (YAP) functions as a tumor suppressor in breast. Cell Death Differ 15:1752-1759.

95. Bertini, E., T. Oka, M. Sudol, S. Strano, and G. Blandino. 2009. YAP: at the crossroad between transformation and tumor suppression. Cell Cycle 8:49-57.

96. Zender, L., M. S. Spector, W. Xue, P. Flemming, C. Cordon-Cardo, J. Silke, S. T. Fan, J. M. Luk, M. Wigler, G. J. Hannon, D. Mu, R. Lucito, S. Powers, and S. W. Lowe. 2006. Identification and validation of oncogenes in liver cancer using an integrative oncogenomic approach. Cell 125:1253-1267.

97. Overholtzer, M., J. Zhang, G. A. Smolen, B. Muir, W. Li, D. C. Sgroi, C. X. Deng, J. S. Brugge, and D. A. Haber. 2006. Transforming properties of YAP, a candidate oncogene on the chromosome 11q22 amplicon. Proc Natl Acad Sci U S A 103:12405-12410.

98. Zhao, B., X. Ye, J. Yu, L. Li, W. Li, S. Li, J. D. Lin, C. Y. Wang, A. M. Chinnaiyan, Z. C. Lai, and K. L. Guan. 2008. TEAD mediates YAP-dependent gene induction and growth control. Genes Dev 22:1962-1971.

99. Bhatia, N., S. Thiyagarajan, I. Elcheva, M. Saleem, A. Dlugosz, H. Mukhtar, and V. S. Spiegelman. 2006. Gli2 is targeted for ubiquitination and degradation by beta-TrCP ubiquitin ligase. J Biol Chem 281:19320-19326.

Vita:

Jia Xu was born on July 16, 1982 in Wuxue city, Hubei, P.R.China, to Minfang Liu and Shaojie Xu. He graduated from Wuxue high school in Wuxue in June of 2000, and pursued his bachelor's degree at Central China Normal University in Wuhan, Hubei. Jia graduated cum laude in June 2004 with a biology degree. He then pursued a master's degree at Wuhan University under the direction of Dr. Yuanyang Hu where he isolated and identified a new nodavirus. He graduated with his master's in Microbiology in June 2006 and immediately entered the University of Texas Health Science Center at Houston, Graduate School of Biomedical Sciences. He completed rotations in the laboratories of Drs. Yinhua Yu, Jean Pierre Issa, and Shiaw-Yih Lin, and joined Dr. Yu's group in June of 2007. Jia was appointed as a pre-doctoral fellow by the Department of Defense, Breast Cancer Research Program from 2010 to 2013.